November 2015

Ingeborg Klarenberg
Master's thesis, 30 ECTS

MSc programma Sustainable Development
Track Gobal Change & Ecosystems
Utrecht University

Microbial community dynamics and extracellular enzyme activities in modern and ancient carbon dominated waters in northest Siberia

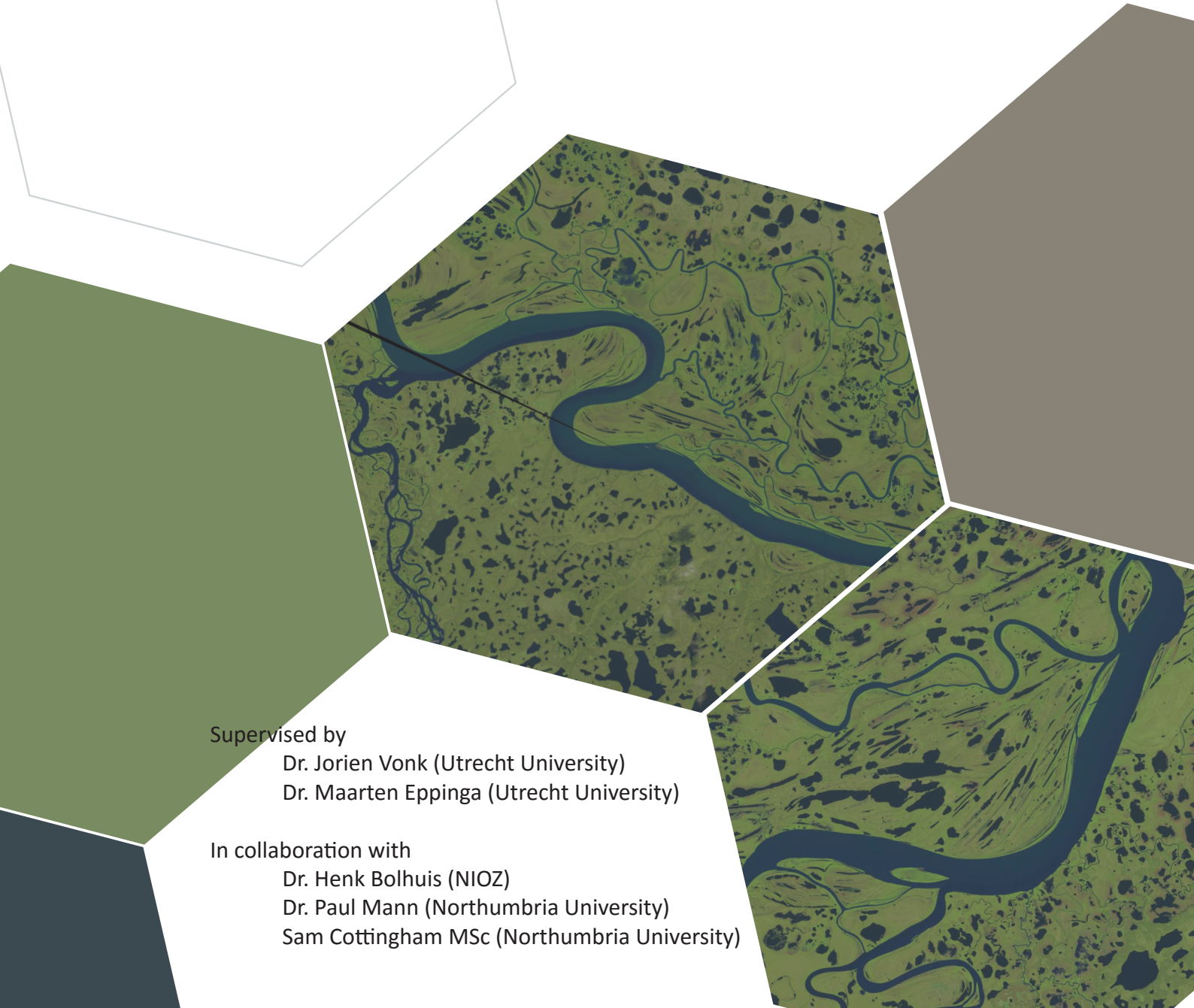

Supervised by
Dr. Jorien Vonk (Utrecht University)
Dr. Maarten Eppinga (Utrecht University)

In collaboration with
Dr. Henk Bolhuis (NIOZ)
Dr. Paul Mann (Northumbria University)
Sam Cottingham MSc (Northumbria University)

Abstract

Permafrost thaw in the arctic as a result of climate change, leads to the transport of organic matter from terrestrial to fluvial networks. Part of this organic matter is mobilized from Pleistocene aged Yedoma permafrost and is highly labile. The degradation of this organic matter can enhance the positive feedback between permafrost melt and the climate system. Therefore it is important to understand the processes involved in its breakdown. Here microbial communities and potential extracellular enzyme activities in aquatic environments dominated by ancient and modern carbon in northeast Siberia were compared.

A seven-day incubation experiment was done to assess the change in microbial communities and enzyme activities during the degradation of organic matter in ancient organic matter and modern organic matter waters. Bacterial and Archaeal communities were assessed using denaturing gradient gel electrophoresis (DGGE) of PCR-amplified 16S gene fragments. The activities of three hydrolytic enzymes were measured using fluorescent substrates in high throughput microplate assays. The activity of phenol oxidase was measured in the same way using colorimetric microplate assays.

Some differences in microbial richness and diversity were found as well as diverse bacterial communities between the compared sites. Also, the particle associated bacteria showed a different response to incubation than the free living bacteria. However due to methodological constraints, no hard conclusions could be drawn from the PCR-DGGE analysis.

In contrast to earlier studies on dissolved organic matter (Mann et al. (2013) and Vonk et al. (2013b), high phenol oxidase activities as well as hydrolytic enzyme activities were found in ancient permafrost degradations. For the Kolyma river, no phenol oxidase activities were detected, while hydrolytic enzyme activities increase, indicating nutrient limitation. Y3 showed no phenol oxidase activities and a decrease in hydrolytic enzyme activities. In this study enzyme activities were in fact assessed on particulate matter instead of dissolver organic matter. The particulate fraction in these environments might thus have a different phenolic content than the dissolved fraction. There also the metabolic mechanisms involved in that breakdown of the particulate organic material might be different than for the dissolved organic material.

Table of contents

List of tables

List of Figures

List of abbreviations

DGGE	Denaturing Gradient Gel Electrophoresis
DNA	Deoxyribonucleic Acid
DY	Duvanni Yar
EEA	Extracellular Enzyme Activity
Kol	Kolyma
PCR	Polymerase Chain Reaction
rRNA	Ribosomal Ribonucleic Acid
OTU	Operational Taxonomic Unit

1. Introduction

The global carbon cycle is currently being influenced by human activity through burning of fossil fuels and land-use change (IPCC 2014, Schuur et al. 2008). This releases greenhouse gases (CO_2, CH_4) that change the heat-trapping capacity of the earth's atmosphere and thereby change the earth's climate (IPCC 2014). Natural fluxes of carbon from terrestrial and marine reservoirs are an order of magnitude larger annually than the carbon released from fossil fuels and land-use change (Schuur et al. 2008). Therefore, small changes in the processes that lead to the natural release of greenhouse gases from terrestrial carbon pools can lead to huge changes in the amount of atmospheric carbon (Schuur et al. 2008).

One of the terrestrial carbon pools from which greenhouse gases are released is permafrost, which can be defined as subsurface material being frozen for at least two successive years, although some of the organic material is stored in permafrost for thousands of years. The estimated size of the carbon pool stored in northern circumpolar permafrost lies between 1330-1580 GT carbon (Schuur et al. 2015), which is more than twice the size of the entire atmospheric carbon pool (Schuur et al. 2008). Global climate models predict an increase in temperatures of 3 to 9 °C in the high latitudes by the end of the 21st century (IPCC 2014). Higher temperatures lead to permafrost thaw, and decomposition of its organic matter to greenhouse gases, which can form an important potential positive feedback from terrestrial ecosystems to the atmosphere (Schuur et al. 2008). The most important process by which carbon is released to the atmosphere is microbial decomposition, which is also expected to increase when the temperature rises (Schuur et al. 2008). Microbial decomposition depends on the quality of the organic substrate, temperature, moisture availability, nutrient availability and oxygen availability (Schuur et al. 2008). In anaerobic soils microbes release CO_2 and the much stronger greenhouse gas CH_4, whereas in aerobic conditions only CO_2 is released. Cumulative carbon emissions however have been shown to be about 80 % lower from anaerobic soils (Schuur et al. 2015). Furthermore, in addition to CO_2 and CH_4, the greenhouse gas N_2O can be released by microbial activity (Graham et al. 2012).

Schuur et al. (2015) estimate that 5-15 % (10 % is equivalent to 130-160 Pg carbon) of the permafrost carbon pool is at risk to be released into the atmosphere in this century, which is comparable to the amount of carbon loss due to land-use change in the tropics (Schuur et al. 2008). However, a detailed and mechanistic understanding of the key processes in carbon and nitrogen cycling related to permafrost thaw does not yet exist (Graham et al. 2012).

As a result of temperature increase, shifts in microbial communities that produce extracellular enzymes that are able to optimize soil organic matter degradation can be expected, which could result in a larger positive feedback to the atmosphere (Graham et al. 2012, Jansson and Taş 2014). This has been illustrated by Mackelprang et al. (2011) showing that during the transition from frozen to thawed permafrost rapid shifts in microbial composition occur and changes in functional gene abundances, such as enrichments in genes involved in the transport and metabolism of specific carbohydrates. Crump et al. (2012) discovered that a substantial part of the bacterial and archaeal diversity in arctic surface freshwaters originate from upstream complex soil environments, indicating that these upstream terrestrial settings act as important pools and sources for microbial diversity in downstream surface waters.

The microbial breakdown of organic matter in permafrost is regulated by its composition as well as nutrient availability. Extracellular enzymes allow microbes to break down complex organic compounds into smaller molecules. The stoichiometry of extracellular enzyme activities (EEAs) can indicate relative nutrient limitations on microbial assemblages (Hill et al. 2012). Commonly measured EEAs include glucosidase (involved in the degradation of cellulose and hydrolyses glucose from cellobiose), alkaline phosphatase (hydrolyses phosphate from phosphosaccharides and phospholipids), N-acetylglucosaminidase (hydrolyses glucosamine from chitobiose) and leucine aminopeptidase (hydrolyses leucine and other hydrophobic amino acids from the polypeptides) (Sinsabaugh et al. 2009). Furthermore, oxidative enzymes (such as phenol oxidase) are able to cleave the aromatic nuclei of phenolic compounds as for instance abundant in lignin (Sinsabaugh 2010, Mann et al. 2013). Mann et al. (2013) show that high concentrations of phenolic compounds in modern dissolved organic matter inhibit enzyme synthesis or activity of bacteria and thereby limit organic carbon degradation in Arctic river waters. Ancient permafrost carbon is suggested to contain relatively little phenolic compounds and is thus preferred over modern carbon by microbes when it is mobilized into fluvial systems (Mann et al. 2013). This could be an explanation for the finding that the major part of the dissolved organic carbon in arctic rivers seems to originate from modern sources (Spencer et al. 2015).

During the late Pleistocene, loess deposits with an average of about 25 m have accumulated in Northeast Siberia and in parts of Alaska and Northwest Canada, which were not covered by glaciers. This ancient, organic-rich form of permafrost (Yedoma) contains about 450 GT carbon (~25 % of total carbon in permafrost soils) and decomposes quickly when thawed and compared to modern boreal and tundra soils of high carbon lability (Zimov et al. 2006a, Zimov et al. 2006b). Streams and rivers draining and eroding Yedoma permafrost contain organic material which is highly biologically reactive (Vonk et al. 2013a). This ancient permafrost carbon has a lower dissolved phenolic content than modern organic carbon and is therefore more susceptible to microbial degradation (Mann et al. 2013). In addition, a peak in activity of ancient microbes originating from permafrost could add to the quick microbial degradation (Rivkina et al. 1998). Krivushin et al. (2015) report significant differences in microbial genera from ancient (±30.000 years) permafrost sediments sampled at different sites in the Kolyma-Indigirka Lowland in northeast Siberia. The most abundant genera were *Mycobacterium*, *Bradyrhizobium*, *Rhodopseudomonas* and *Hyphomicrobium* in a Panteleikha lake sediment and *Conexibacter*, *Streptomyces*, *Nakardiodes* and *Frankia* from the Omolon River (tributary river of the Kolyma).

The microbial processing of ancient Yedoma permafrost carbon in streams and rivers may play an important role in the future release of greenhouse gases to the atmosphere. What remains unclear is whether microbial communities and EEAs are different for ancient carbon dominated waters compared to modern carbon dominated waters. To answer this question, this used PCR-DGGE to study differences in microbial community composition from a fluviatile environment in northeast Siberia containing modern and ancient carbon. The activity of four extracellular enzymes was determined using microplate assays.

2. Research questions and hypotheses

The aim of this research will be to determine whether microbial communities and EEAs degrading Yedoma permafrost in Northeast Siberia are different from those degrading modern carbon. This question will be answered by addressing different sub questions:

1. What is the composition of the bacterial and archaeal communities?
    a. Are they similar or different in old and modern permafrost degradations?
    Hypothesis: Old and modern permafrost are expected to show different bacterial and archaeal communities, since the environmental factors differ between sites (table 1). Archaeal communities are less rich than bacterial communities (Jansson and Taş (2014).
    b. Do the bacterial and archaeal communities change in richness, diversity and composition after a 7-day incubation experiment?

2. Are Yedoma-degradations nutrient limited?
    a. Which extracellular enzymes are most active before and after incubation?
    Hypothesis:
    <u>Before incubation</u>: ancient permafrost carbon is expected to contain relatively little phenolic compounds and therefore, we can expect phenol oxidase to be low in activity and higher activities of enzymes responsible for nutrient release.
    Samples containing modern carbon are expected to have higher phenol oxidase activities and lower activities of enzymes responsible for nutrient release as a consequence of phenolic constraints.
    <u>After incubation</u>: ancient permafrost carbon might become limited in nutrients and thus increases in enzymes responsible for nutrient release could be expected.
    Samples containing modern carbon might show decreases in phenol oxidase activity when phenolic constrains have been removed and if nutrient availability is limited enzymes responsible for nutrient release will increase in activity.

3. Methods

3.1 Sites, samples and environmental variables

In June 2013, water samples of three different sites (Table 1) near Cherskiy in northeastern Siberia (Figure 1) have been collected and environmental variables have been measured during the annually aquatic survey of the Polaris Project (www.thepolarisproject.org/data). At each site, two sample bottles were collected. One sample was filtered the same day in four different size fractions (0.22, 0.45, 1.2, 12 µm pore size) for DNA extraction and enzyme analysis. The other sample was incubated for 7 days at 20 °C to see if the microbial populations decrease or change over time and if and how extracellular enzyme activities change. After incubation the second sample was filtered over the same size fraction as the first part.

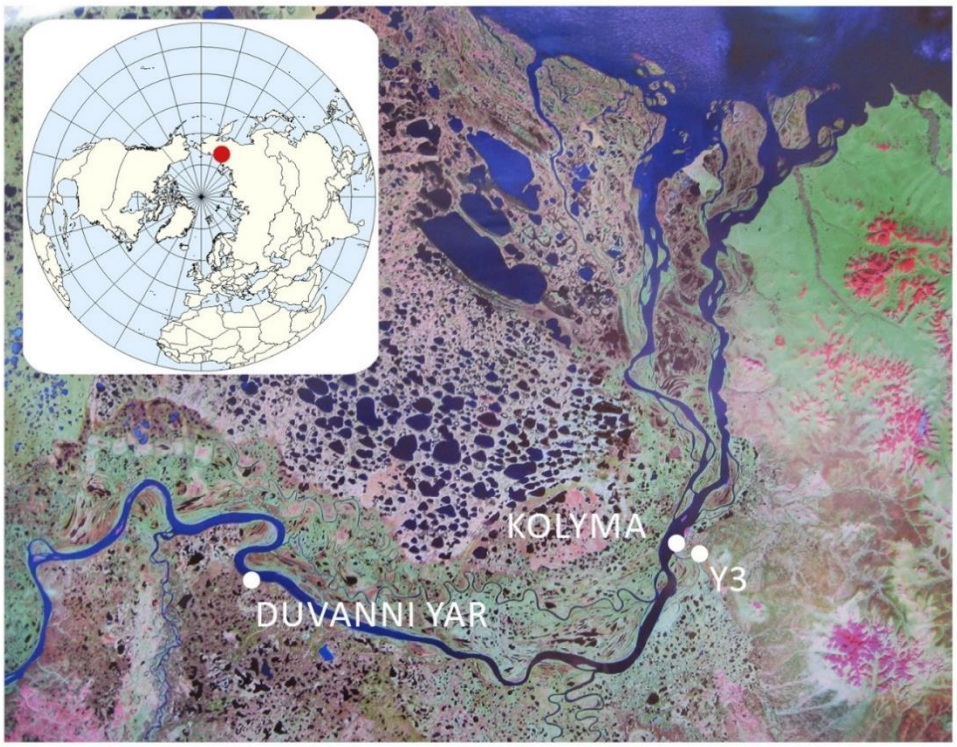

FIGURE 1 LOCATION OF RESEARCH AREA AND THE THREE SAMPLE SITES DUVANNI YAR, KOLYMA AND Y3 (SOURCE SATELLITE IMAGE UNKNOWN, BUT SEE MANN ET AL. (2012)).

Site descriptions

Duvanni Yar is of a Yedoma permafrost exposure (containing sediments that were deposited between 45,000 and 13,000 y ago; Vasil'chuk and Vasil'chuk, 1997) along the Kolyma river. Samples were taken from small thaw streams draining the exposure. This mildly alkaline thaw water is very rich in dissolved organic matter (DOM) compared to the other sites (Table 1).

The second site was the Kolyma river near Cherskiy. The Kolyma represents the largest river on earth draining a watershed of 652924 km^2 by continuous permafrost. Compared to the two other sites, Kolyma has the highest water temperature, but the lowest amount of DOM.

The third site was the Y3-stream: small creek draining a watershed of 17 km^2 upland taiga terrain near Cherskiy containing mostly modern carbon. Y3 is richer in DOM than Kolyma, but less rich Kolyma and has slightly acidic waters.

TABLE 1 SITE DESCRIPTIONS, LOCATIONS AND ENVIRONMENTAL VARIABLES MEASURED IN THE SUMMER OF 2013.

Location Name	Type	Latitude	Longitude	Water Temp	DO	DO	Sp Cond	pH	DOC	TDN	H2O	H2O
		dec deg	dec deg	C	% sat	mg/L	µs/cm		mg C/L	mg N/L	$\delta^{18}O$	$\delta^{2}H$
Y3 above the road	Stream	68,76005	161,45054	9,1	93	10,5	78	6,4	22,5	1,1	-20,41	-155,74
Kolyma at Cherskii	River	68,75424	161,30297	11,7	91	9,8	38	7,5	5,7	0,7	-21,91	-167,52
Duvanni Yar stream 1	Ice Wedge melt water stream			0,8	59	8,3	11	8,1	122,6	6,9	-29,08	-224,71
Duvanni Yar stream 2	Ice Wedge melt water stream	68,63042	159,15042	-	-	-	-	-	73,0	3,6	-29,07	-227,30

Duvanni Yar stream 1 and 2 are located next to each other and are shown here to indicate average values for the environmental variables. Our Duvanni Yar sample originates from stream 2.

In total we collected samples from 3 (sites) * 4 (size fractions) * 2 (before and after incubation) * 3 (replicates) which together give a total of 72 samples.

3.2 Microbial community composition

Bacterial and archaeal communities of each site before and after incubation were described through 16S rRNA gene analysis and denaturing gradient gel electrophoresis (DGGE) as described by Muyzer et al. (1993). DGGE is a molecular fingerprinting technique that separates 16S rRNA gene fragments from different prokaryotic species based on their GC-content. This allows a quick assessment the diversity of gene fragments (Bertrand et al. 2015).

3.2.1 DNA extraction

First, the total DNA was extracted from two replicate filter of the different size fractions from each site. Some filters were absent, and some samples were filtered on more than two filters. DNA was extracted from each separate filter by cutting them into small pieces with a sterile blade and applying the fragments to a PowerLyzer PowerSoil DNA Isolation Kit (Mo Bio Laboratories Inc.) following the manufacturer's instructions for maximum yield. The bead beating was reduced to 7 minutes instead of 10 in order to prevent fragmentation of the DNA (see Appendix 3 for the protocol). The DNA was eluted in 30 µl elution buffer. The nucleic acid concentration and quality were determined with a NanoDrop ND-1000 spectrophotometer.

3.2.2 16S rRNA gene amplification

TABLE 2 OLIGONUCLEOTIDES USED FOR DNA AMPLIFICATION.

Oligonucleotide	Sequence (5' to 3')
Forward Bac-F968-GC	CGC CCG GGG CGC GCC CCG GGC GGG GCG GGG GCA CGG GGG G CCT ACG GGA GGC AGC AG
Reverse U1401R	CGG TGT GTA CAA GAC CC
Forward A2F	TTC CGG TTG ATC CYG CCG GA
Reverse U1492R	GGT TAC CTT GTT ACG ACT T
Forward SAF341F	CTA YGG GGC GCA GCA GG
Reverse PARCH519R-GC	CGC CCG GGG CGC GCC CCG GGC GGG GCG GGG GCA CGG GGG G ACC AGA CTT GCC CTC C

For the DGGE analysis, the 16S rRNA gene fragments were amplified by polymerase chain reaction (PCR) using specific primers for the bacterial and archaeal fraction. For bacteria the primer F968-GC, containing the GC clamp was combined with the reverse universal U1401R (Table 2) in a touchdown PCR. In a touchdown PCR, the annealing temperature is gradually decreased, which increases the specificity of the reaction. A PCR reaction mixture of 50 µl was used (Table 3). The PCR reaction conditions were: an initial polymerase activation step for 3 minutes at 95 °C; 10 cycles of 95 °C for 1 minute, a touchdown from 60-55 °C for 1 minute (each cycle the temperature was decreased with 0.5 °C) and elongations at 72 °C for 1 minutes; 35 cycles of 95 °C for 1 minute, 56 °C for 1 minute and 72 °C for 1 minute; followed by 72 °C for 30 minutes (Table 3). Randomly selected samples were put on a 1.5 % agarose gel and compared with a mass ruler (Thermo Fisher) to verify the size of the PCR products.

The PCR products were purified with an E.Z.N.A. Cycle Pure kit and diluted in 25 µl elution buffer. The nucleic acid concentration of all purified samples was quantified with a NanoDrop ND-1000 spectrophotometer.

For the archaeal DGGE PCR reaction a nested PCR was performed, as the archaeal DNA concentrations were low after several PCR tests. The nested PCR consisting of a general archaeal 16S rRNA gene amplification using the archaeal forward primer A2F and the universal U1492R reverse primer followed by a DGGE specific PCR with the SAF341F and PARCH519R-GC primers set (Table 4). For the first PCR, a reaction volume of 25 µl was used. The program was as follows: 95 °C for 2 minutes; 25 cycles of 94 °C for 1 minute, 50 °C for 1 minute, 72 °C for 1 minute; 72 °C for 7 minutes (table 4). A random selection of samples was run on a 2.5 % agarose gel in order to determine successful amplification. The products were purified and quantified as described above.

Two microliters of the purified PCR products were used as DNA-template DGGE specific PCR.

The program for the nested PCR was 95 °C for 3 minutes; 10 cycles of 95 °C for 1 minute, a touchdown from 55 to 50 °C for 1 minute, 72 °C for 1 minute; followed by 40 cycles of 95 °C for 1 minute, 50 °C for 1 minute, 72 °C for 1 minute; 72 °C for 30 minutes (Table 4).

The PCR products were purified and quantified as described above.

TABLE 3 PCR REACTION MIXTURE AND PROGRAM FOR BACTERIA 16S DGGE

Reagent	Final Concentration
DTW	
Template	2 µl
PCR buffer (incl. 1.5 mM $MgCl_2$)	1 x
DMSO	2.5 %
dNTP's	0.2 mM
Bac-F968-GC (008-053)	0.2 µM
U1401R (006-066)	0.2 µM
GE Taq polymerase	0.04 U/ul

Program	Temperature	Time
Act. Taq	95 °C	3 min
10x	95 °C	1 min
	60-55 °C	1 min
	72 °C	1 min
35x	95 °C	1 min
	56 °C	1 min
	72 °C	1 min
	72 °C	30 min

TABLE 4 PCR REACTION MIXTURE AND PROGRAMS FOR ARCHAEA 16S AND ARCHAEA 16S DGGE

Reagent	Final concentration Archaea 16S	Final concentration Archaea 16S DGGE
DTW		l
Template	1.00 µl	2.00 µl
PCR buffer (incl. 1.5 mM $MgCl_2$)	1x	1x
BSA	0.01 %	-
DMSO	5.00 %	2.50 %
dNTP's	0.20 mM	0.20 mM
A2F	0.20 µM	-
U1492R	0.20 µM	-
SAF341F	-	0.20 µM
PARCH519R-GC	-	0.20 µM
GE Taq polymerase	0.04 U/ul	0.04 U/ul

Program PCR Archaea 16S		
Act. Taq	95 °C	2 min
15x	94 °C	1 min
	50 °C	1 min
	72 °C	2 min
	72 °C	7 min

Program PCR Archaea 16S DGGE		
Act. Taq	95 °C	3 min
10x	95 °C	1 min
	55-50 °C	1 min
	72 °C	1 min

40x	95 °C	1 min
	50 °C	1 min
	72 °C	1 min
	72 °C	30 min

3.2.3 Denaturing gradient gel electrophoresis

For archaea and bacteria, two 8 % polyacrylamide gels were run in 1 x TAE buffer using an Ingeny PhorU-2 system (Ingeny, Goes, NL). For the bacteria, the denaturant ranged from 45 % to 60 % to obtain optimal fragment separation. For the archaea, the denaturant ranged from 45 % to 65 %. This gradient was created following the instructions of the manufacturer. To induce polymerization, 50 µl of 20 % ammonium persulphate (APS) and 5 µl tetramethylethylenediamine (TEMED) were added to the formamide-urea-arcylamide solution. After 1 hour of polymerization, a stacking gel consisting of 8 % acrylamide and 0.5 x TAE-buffer, 60 µl of 20 % APS and 6 µl TEMED was pipetted on top of the gradient gel.

All samples were diluted to 200 ng DNA per 20 µl of Milli-Q water in order to be able to compare the band intensities with each other. 2 µl of loading dye was added to the samples and applied to the gel. A marker was included for normalization of the lanes and comparison of multiple gels. The electrophoresis was run at 60 °C and 100V for 18 hours.

After electrophoresis, the gels were silver stained using an automated gel stainer (Hoefer Processor Plus, Amersham Biosciences) and scanned with an Epson Perfection V700 photo scanner. The gel staining program was as described in table 5.

TABLE 5 SILVER STAINING SOLUTIONS AND PROGRAM

Step	Action	Solution (200 ml)	Time
1	Fixation	0.05 v/v % acetic acid 10 v/v % ethanol 96 %	30 min
2	Staining	0.2 w/v % silver nitrate solution	15 min
3	Washing	Milli-Q water	1 min (3x)
4	Developing	1.5 w/v % sodium hydroxide 0.15 v/v % formaldehyde	5 min
5	Stopping	0.75 w/v % sodium carbonate	5 min
6	Conservation	10 v/v % glycerin 25 v/v % ethanol	7 min

3.2.4 Community fingerprint analysis

The banding patterns of the DGGE gels were normalized (using the marker lanes) and quantified with BioNumerics software version 6.6 (Applied Maths, Kortrijk, Belgium). Lanes were defined, the background was subtracted and a correlation matrix was calculated. Cluster analysis to determine whether bacterial community compositions are similar or not was done with Pearson correlation and the unweighted pair group method using arithmetic means (UPGMA). The band matching matrix with quantitative band information was used for further statistical analysis using the library package 'vegan' (Version 2.3-0) (Oksanen et al. 2015) in R (R Development Core Team, 2015). The Shannon species diversity index (based on the number and the intensity of the bands) (Equation 1), the Chao species richness index (estimator of

the total number of species, based on the number of rare classes) (Equation 2) and the number of Operational Taxonomic Units (OTUs, based on the number of bands) were calculated.

EQUATION 1 *SHANNON INDEX*

$$H' = -\sum_{i=1}^{R} p_i \ln p_i$$

H' = Shannon's diversity index
R = total number of species in the community
p_i = proportion of R made up of the i^{th} species

EQUATION 2 *CHAO1*

$$S_{chao1} = S_{obs} + \frac{n_1(n_1 - 1)}{2(n_2 + 1)}$$

S_{chao1} = estimated richness
S_{obs} = observed number of species
n_1 = the number of operational taxonomic units (OTUs) with only one sequence ('singletons')
n_2 = the number of OTUs with only two sequences ('doubletons')

3.2.5 Statistical analysis

Constrained correspondence analysis (CCA) was applied to the DGGE results in order to investigate the effect of site, incubation and filter size on the variance in the microbial communities and to see whether the communities of the different sites are similar together or not. The significance of these factors was assessed with Anovas. All statistics were conducted using R.

3.3 Extracellular enzyme assays

Extracellular enzyme activities of three hydrolytic and one oxidative enzyme were measured using specific chromogenic/fluorescent substrates (table 6) in microplate assays.

Microplate assays allow for a quick analysis of large numbers of samples as well as comparison between spatially separated sites (Jackson et al. 2013). The remaining filters from each site were used for the assays. In order to extract material from the filters, they were immersed in 10 mL deionized water for about 12 hours. The first 1 to 4 hours the samples were gently shaken to help the material get extracted from the filter. The enzyme activities of Phos, ß-gluc, and NAGase were determined through fluorescence assays (see 3.3.1) whereas the enzyme activity of PhOx was determined through absorbance (see 3.3.2).

TABLE 6 ENZYMES, THEIR FUNCTION AND SUBSTRATES

Enzyme	Function	Substrate
Phenol Oxidase (PhOx)	Degradation of lignin	L-dihydroxyphenylalanine
Alkaline Phosphatase (Phos)	Releases ester-bound phosphate	4-MUB-phosphate
ß-glucosidase (ß-gluc)	Releases glucose from cellulose decomposition	4-MUB-β-glucopyranoside

N-actelyglucosaminidase (NAG)	Degradation of chitin	4-MUB-N-acetyl-β-D-glucosaminide

3.3.1 Fluorometric assays

The fluorescent assays were conducted following the method for extracellular enzyme activity in natural waters of Jackson et al. (2013). 4-methylumbelliferone (MUB) linked substrates were used for the assays (phosphatase (Phos), ß-glucosidase (ß-gluc), N-acetylglucosaminidase (NAG)) (table 6). 200 µM solutions of the MUB-linked substrates were prepared, by dissolving the substrates in autoclaved distilled H_20 in sterile 50 ml tubes. These tubes were then wrapped in aluminum foil to protect the solutions from light and stored at 4 °C. Light can cause instability of MUB (Bell et al. 2013).

A stock solution of MUB standard was prepared by making a solution of 100 µM 4-methylumbelliferone in distilled H_20. This solution was wrapped in aluminum foil and stored at 4 °C. Immediately before use, the 100 µM stock solution was diluted by 1/10 in autoclaved H_20 to make a working solution of 10 µM.

A stock solution of 100 mM bicarbonate buffer was prepared by dissolving 8.4 g of $NaHCO_3$ into 1 L distilled H_20. The working solution of 5mM was made by diluting the stock solution by 1/20 into distilled H_20.

Black 96-well microplates were used for the assays in order to prevent light affecting the substrate. The microplates were organized following the instructions of Jackson et al. (2013) as shown in Figure 2a en Figure 2b. The light was dimmed before the light-sensitive MUB-linked substrate was added. After adding the substrates, the microplates were placed in a dark box.

The fluorescence was read with a 96-well plate reader (Biotek Synergy 2 Multi-Mode Reader) and digitized with Gen5 Data Analysis Software (Biotek), using a 360 nm, 40 nm bandwidth excitation filter and a 460 nm, 40 bandwidth emission filter at a sensitivity setting of 45. During the first half hour, measurements were taken every 5 to 10 minutes. Then the time steps were increased to 15 minutes and later 30 minutes. Measurements were taken up to approximately 4 hours after adding the substrate.

In order to convert measured fluorescence intensity to enzyme activity (in nmol ml^{-1} hr^{-1}) the following formula was used (Jackson et al. 2013):

EQUATION 3 ENZYME ACTIVITY (FLUOROMETRIC ASSAY)

$$\textit{Enzyme activity } (mol\ hr\text{-}1\ ml\text{-}1) = \frac{(mean\ sample\ fluorescence) - (mean\ initial\ sample\ fluorescence)}{\left(\frac{mean\ standard\ fluorescence}{0.5\ mol}\right) \times \left(\frac{mean\ control\ fluorescence}{mean\ stanard\ fluorescence}\right) \times (time\ in\ hr) \times (0.15\ ml)}$$

The activity was calculated between the measurement at 40 minutes after the start and the last measurement as the increase in fluorescence was linear between these readings.

3.3.2 Colorimetric assay

For the colorimetric assay (phenol oxidase (PhOx)) the "Phenol Oxidase and Peroxidase Assays" (Colorado State University, 2012) protocol was used (Appendix 1). For the PhOx assay, L-3,4-dihydroxyphenylalanine

(L-DOPA) was used as a substrate. A 25 mM solution of L-DOPA was prepared in 50 mM acetate buffer of pH 5.0. This substrate was freshly prepared before running the assay.

A 96-well microplate was used with a similar set-up as used for the fluorometric assays (Figure 2), but without the quenched controls and the standards.

The absorbance was read with a 96-well plate reader (Biotek Synergy 2 Multi-Mode Reader) using a 405 nm filter. The intervals between the measurements were 15 minutes to 30 minutes to an hour. Measurements were taken up to approximately 6 hours after adding the substrate.

In order to convert absorbance into enzyme activity (in µmol ml^{-1} h^{-1}) the following formula was used (Colorado State University, 2012):

EQUATION 4 ENZYME ACTIVITY (COLORIMETRIC ASSAY)

$$Activity\ (\mu mol\ hr\text{-}1\ mL\text{-}1\ ) = \frac{(mean\ OD\ of\ assay\ wells) - (mean\ OD\ of\ blank\ wells) - (mean\ OD\ of\ negative\ control\ wells)}{(7.9\ \mu mol\text{-}1) \times (incubation\ time\ in\ hr) \times (0.15\ mL)}$$

OD = optical density or absorbance, which is the logarithm of the ratio between the intensity of incidental and transmitted light.

The activity was calculated between 30 minutes after the start and the last reading, when the increase in absorbance per time step was linear.

3.3.3 Statistical analysis

To identify significant differences in pre- and post-incubation enzyme activities per filter size fraction, t-tests were used. The t-test to compare pre and post incubation activities was only applied if both samples were initially normally distributed and homoscedastic as for some samples activities were zero (below detection limit) and other were not transformable to a normal distribution. All statistical tests were conducted using R. The level of significance used was 0.05.

A

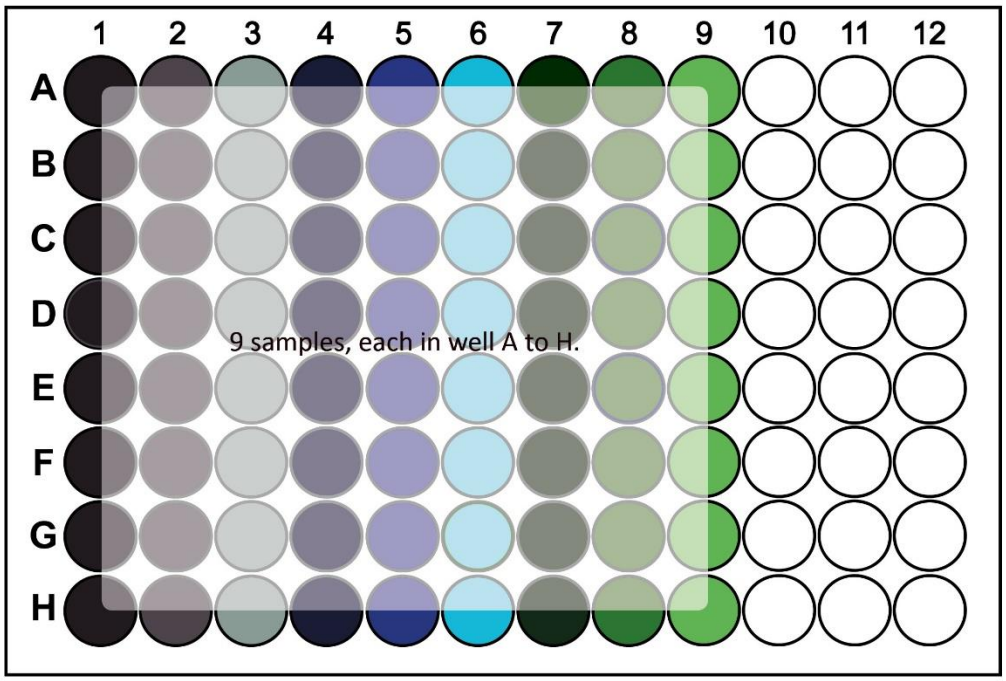

B

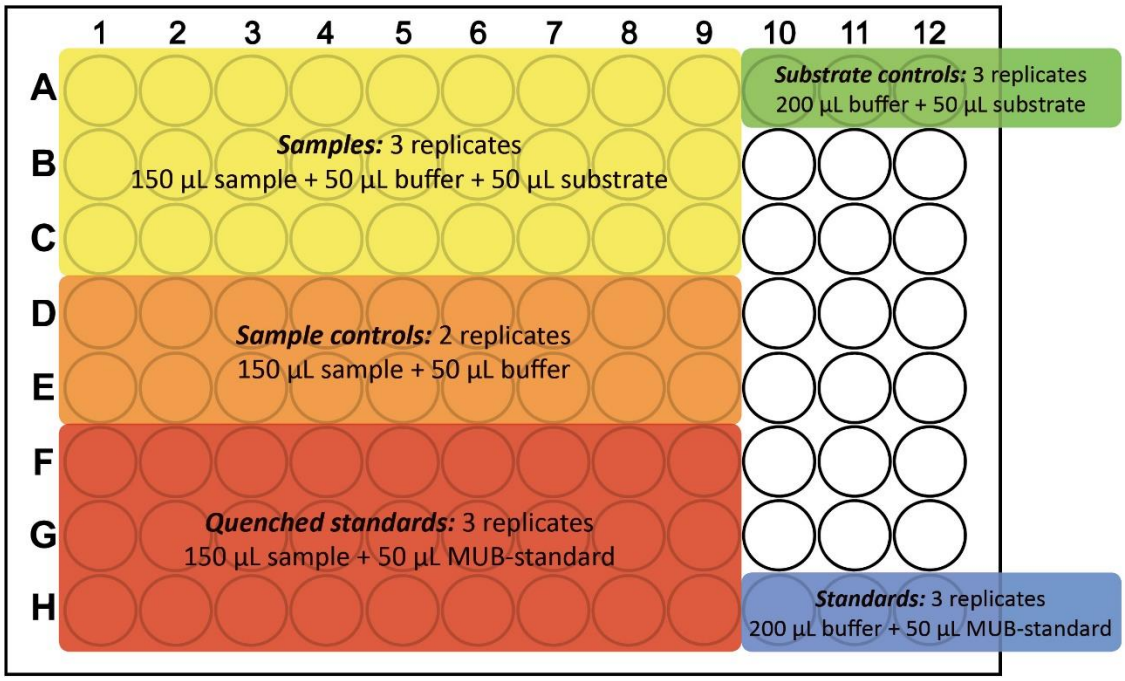

FIGURE 2 LAYOUT OF 96-WELL BLACK MICROPLATES FOR THE ASSAY OF EXTRACELLULAR ENZYME ACTIVITIES IN WATER SAMPLES USING THE FLUOROMETRIC MUB-LINKED SUBSTRATE TECHNIQUE (AFTER JACKSON ET AL. 2013). FOR THE COLORIMETRIC ASSAY, THE SAME SET-UP WAS USED, EXCEPT FOR THE QUENCHED STANDARDS AND THE STANDARDS. A) SHOWS HOW EACH SAMPLE WAS PIPETTED INTO THE WELLS. B) SHOWS THE AMOUNT OF EACH SOLUTION IN THE WELLS.

4. Results

4.1 Bacteria

In this part, the results of the DGGE for the bacteria are described, first addressing the research question about the bacterial richness and diversity before and after incubation followed by the constrained correspondence analysis of bacterial communities in which the composition of communities between sites and before and after incubation are compared.

Two DGGE gels with bacterial 16S rRNA gene amplicons were generated (Figure 3). The markers that were intended to compare the gels were not clearly visible. This forced us to analyse the gels separately. Diverse banding patterns could be observed, with major bands in the higher region with lower denaturant concentration. Additional bands were present in the lower region with higher denaturant concentration. For further analysis, only the region with clearly visible bands in most lanes was compared. On gel 1 (Figure 3A) 5 to 16 DGGE bands were detected per sample (see Appendix A for the band quantification matrix). On gel 2 (Figure 3B) 8 to 18 DGGE bands were detected per sample (see Appendix B for the band quantification matrix).

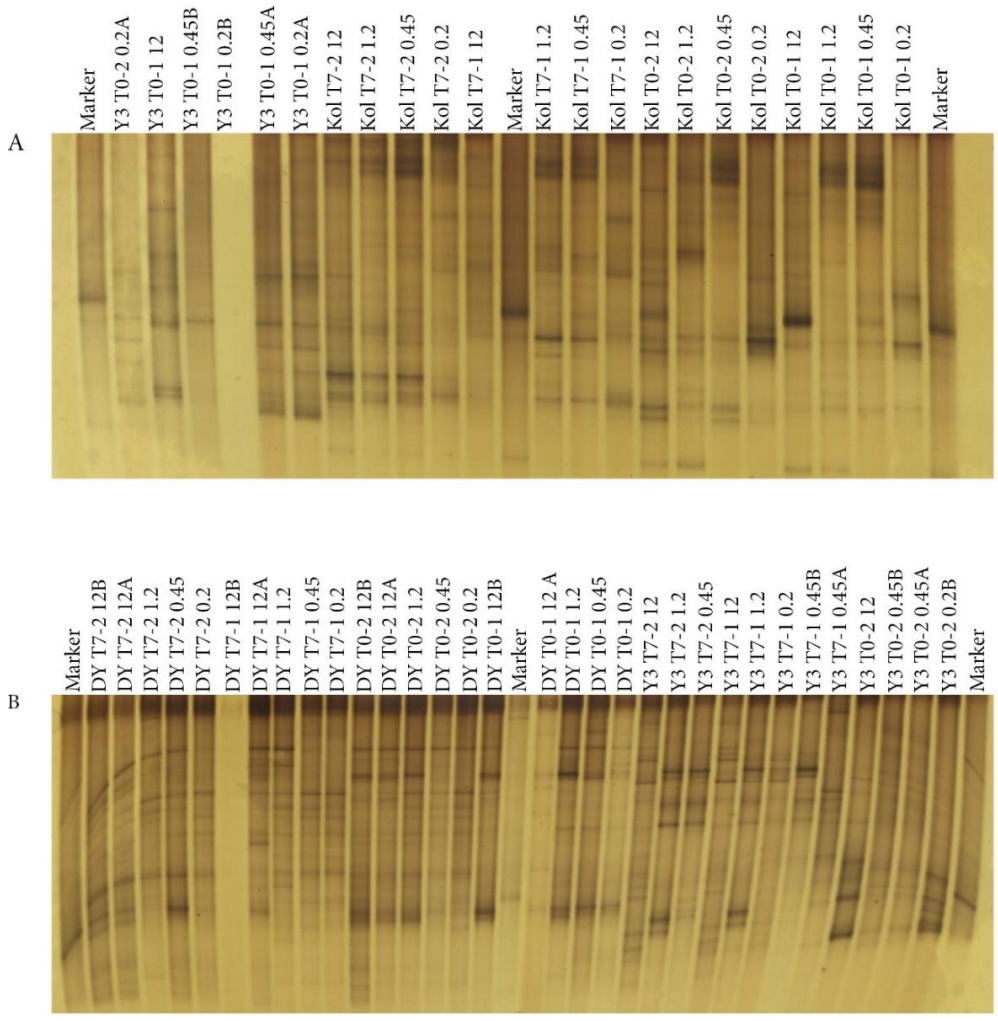

FIGURE 3 DGGE IMAGES OF BACTERIAL 16S RRNA GENE FRAGEMENTS. A) GEL1. B) GEL2.

4.1.1 Bacterial richness and diversity before and after incubation

When considering each band as a unique operational taxonomic unit (OTU) and its density as a measure of OTU abundance, the species richness (number of OTUs) and the Shannon diversity index could be determined (Table 7 and Figure 4). Before incubation Kolyma and Duvanni Yar showed a higher total richness and diversity than Y3, based on the total number of bands of all size fractions (Table 7). After incubation the total richness and diversity increased for Y3 and stayed similar to pre-incubation values for Kolyma and Duvanni Yar. The Chao1 richness estimator indicated a decrease in richness for Kolyma and Duvanni Yar and both an increase (gel1) and a decrease (gel2) for Y3.

Figure 4 shows the number of OTUs (richness) and the Shannon diversity per site per size fraction before and after incubation. As the sample size was small (n = 2), the results were not statistically analysed. The size fractions showed diverse responses to the incubation. Duvanni Yar showed an increase in richness (Figure 4A) after incubation for all fractions. The 0.2 µm factions had on average the highest number of OTUs before and after incubation. The changes in diversity (Figure 4D) after incubation showed the same trends as the number of OTUs. Two post-incubation samples were missing (1.2 and 12 µm filters).

For Kolyma (Figure 4B), the incubation led to a strong increase of OTUs recovered on the 0.2 µm filter. On average, the richness increased for all size fractions. The Shannon diversity (Figure 4E) showed the same increase as the richness, except for the 1.2 µm fractions, for which the diversity decreased slightly after incubation.

For Y3 some filters were missing or could not be used in the analysis (post-incubation 0.2 µm filters and pre-incubation 1.2 µm filters). The 0.45 µm and the 12 µm fractions showed an increase in the number of OTUs after incubation (Figure 4C). The Shannon diversity index showed the same pattern (Figure 4F).

TABLE 7 DIVERSITY INDICATORS FOR BACTERIA FOR KOLYMA, Y3 AND DUVANNI YAR.

Site	**Nr of bands (S)**		**Chao1**		**Shannon (H)**	
	Before inc	After inc	Before inc	After inc	Before inc	After inc
Kolyma	31	32	39.8	36.7	3.04	3.02
Y3	22	32	23.7 / 49.0	40.3	2.78 (gel1) 2.62 (gel2)	3.01 (gel2)
Duvanni Yar	31	33	40.0	35.6	2.90	3.08

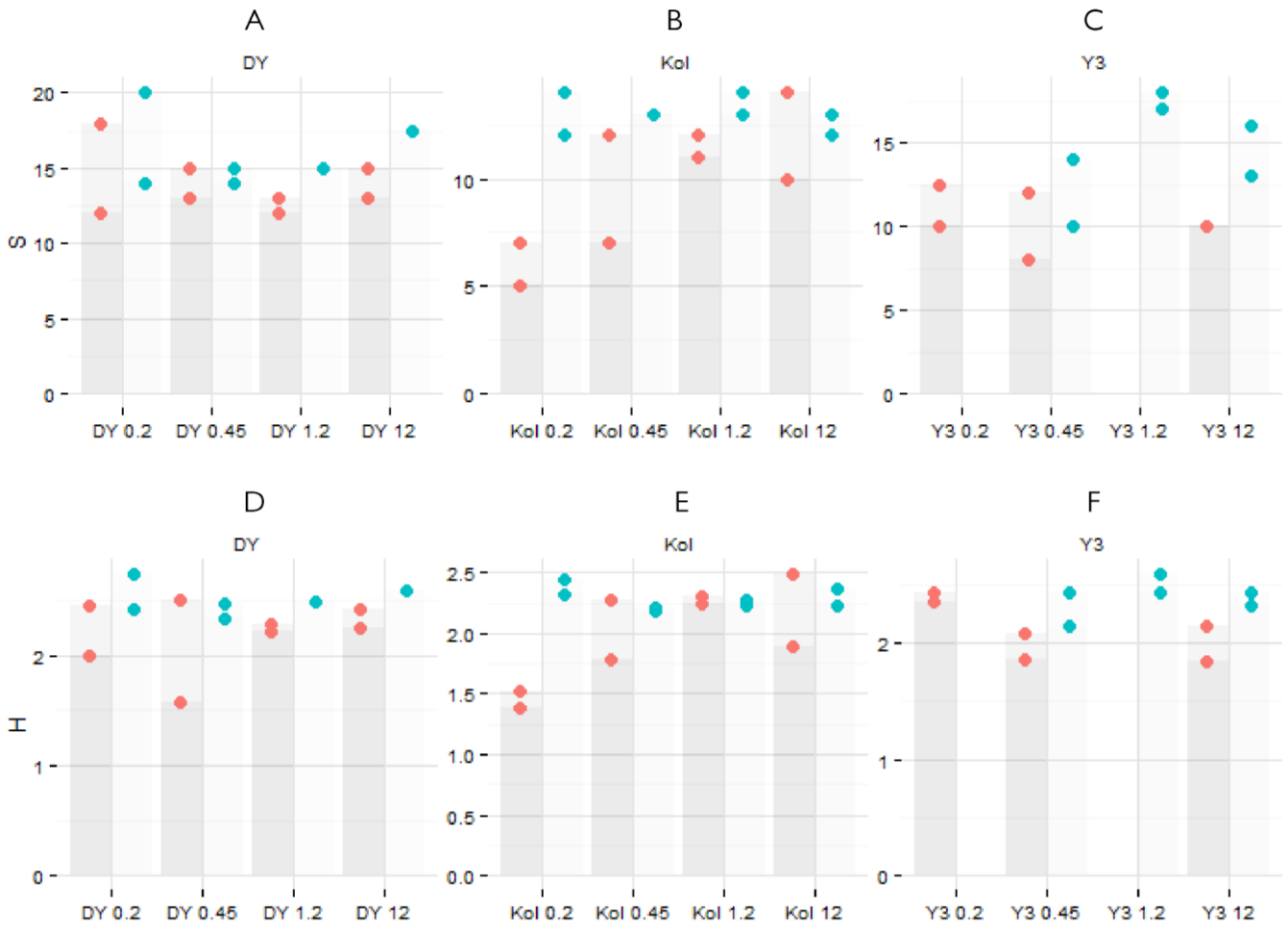

FIGURE 4 NUMBER OF OTUS AND SHANNON DIVERSITY BEFORE AND AFTER INCUBATION FOR EACH FILTER PORE SIZE FOR DUVANNI YAR (A, D), KOLYMA (B, E) AND Y3 (C, F). PER FILTER, THE VALUES OF THE TWO SAMPLES ARE GIVEN; BEFORE INCUBATION IN RED, AFTER INCUBATION IN BLUE.

4.1.2 Cluster analysis

Cluster analysis based on the UPGMA method was used to see how similar the communities of the different sites before and after incubation were. For gel 1 and gel 2, the samples clustered mainly according to site and filter size and to a lesser extent incubation (Figure 5). For gel 1 (Figure 5A), the bacterial communities of Kolyma were similar, especially for the 0.45 and 1.2 µm fractions that formed two clusters corresponding to pre- and post-incubation communities. The 0.2 and 12 µm fractions partly clustered together, but the 0.2 µm fractions showed also similarities with Y3 samples. Clustering of the bacterial communities of Y3 and Duvanni Yar was less clear-cut (Figure 5B). Both Y3 and Duvanni Yar formed clusters that also contained samples from the other site and pre- and post-incubation samples were only partly distinct.

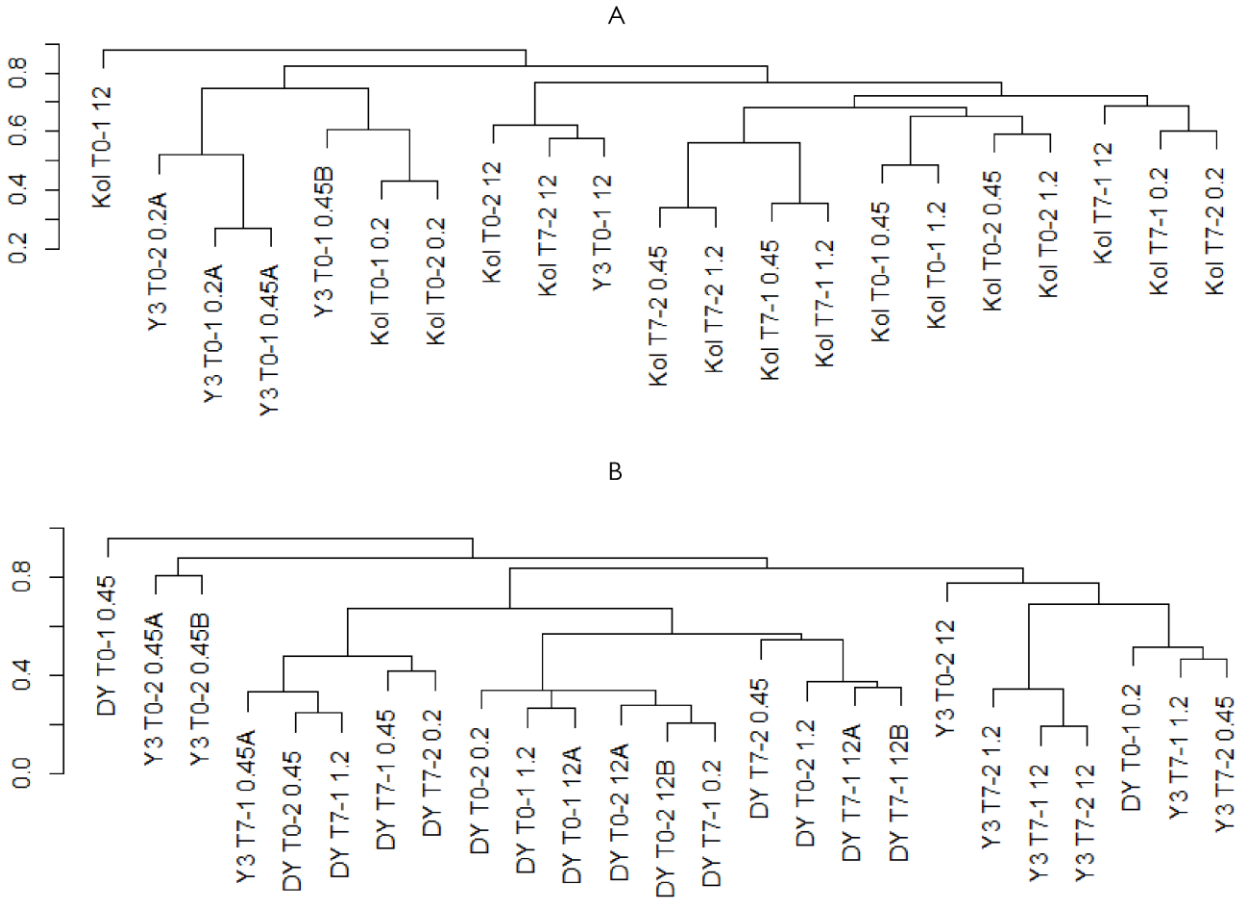

FIGURE 5 UPGMA DENDROGRAMS BASED ON THE DGGE BANDING PATTERN OF BACTERIAL 16S GENE FRAGMENTS. A) GEL 1 AND B) GEL 2.

4.1.2 Constrained correlation analysis of bacterial community composition

The constrained correspondence analysis (CCA) based on the band distance matrix of gel 1 (Figure 6A) revealed three main clusters consisting of the Kolyma pre-incubation samples, the Kolyma post-incubation samples and the Y3 pre-incubation samples. The first two axis of the CCA of gel1 together explained 69.9 % of the variation in the bacterial communities. The first CCA axis explained 38.8 % of the variation and was related to sample site and filter pore size. The second CCA axis explained 31.1 % of the variation and was closely linked to incubation. All three factors showed a significant correlation with the bacterial communities on gel 1: the factor sampling site explained 16.1 % ($p = 0.001$), incubation 13.6 % ($p = 0.002$) and filter size) 13.9 % ($p = 0.002$) (see Appendix E for the CCA statistics).

For gel 2, the CCA (Figure 6B) showed two less distinct clusters of which the first one consisted of Y3 post-incubation samples and the second one of Duvanni Yar pre and post-incubation samples. One of the pre-incubation samples of Y3 was located in the Duvanni Yar cluster and the other two Y3 pre-incubation samples were located outside the two clusters. The first two CCA axis together, explained 83.8 % of the variation in the bacterial community. The first axis explained 60.1 % of the total variation and was closely

linked to the factor site. The second axis explained 22.7 % and was linked to incubation. However, the factor sampling site was the only significant (p = 0.001) factor explaining 20.5 % of the variation

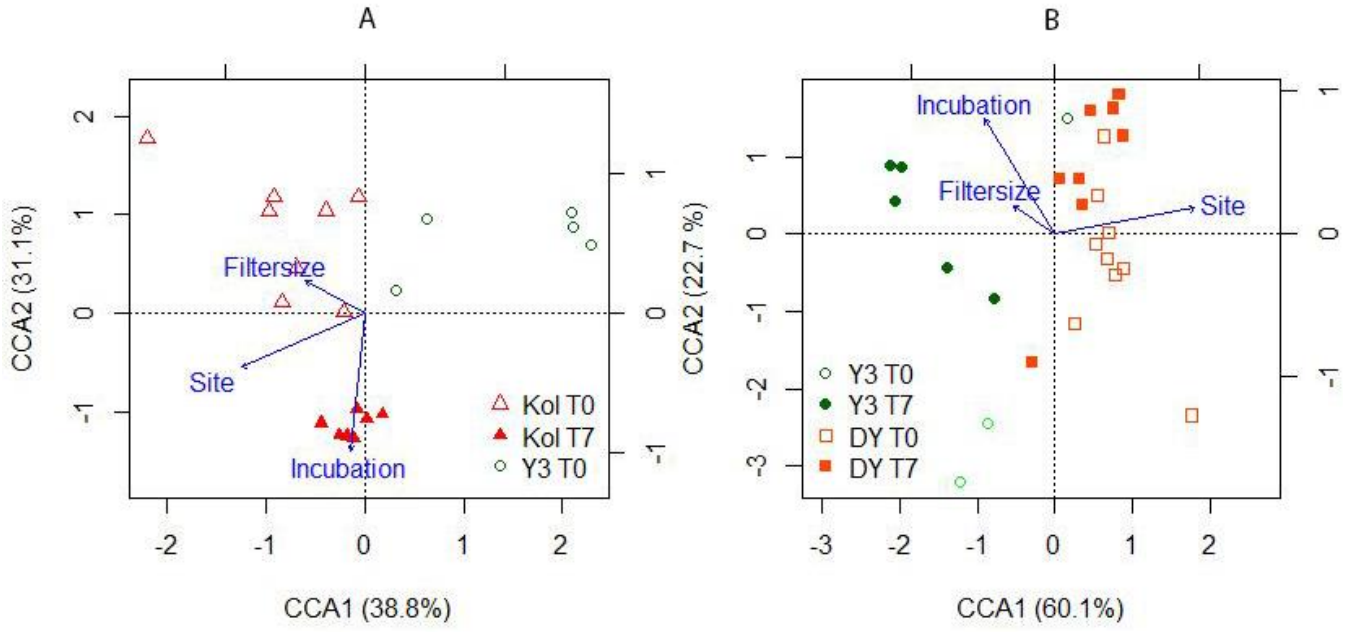

FIGURE 6 CCA ORDINATION PLOT FOR THE FIRST TWO PRINCIPAL DIMENSIONS OF THE RELATIONSHIP BETWEEN BACTERIAL COMMUNITIES OF GEL 1 (A) AND GEL 2 (B) AND SITE, FILTER PORE SIZE AND INCUBATION.

In order to see the how the bacterial communities before and after incubation and the filter pore sizes varied in relation to the factors incubation and filter pore size, CCAs were created of single sites.

Figure 7A shows the CCA of the bacterial communities of the Kolyma. The communities before incubation were more divergent then the communities after incubation that showed a clear cluster. Before incubation the communities of the two 0.2 µm and 1.2 µm fractions clustered, whereas the communities of the two 0.45 µm and 12 µm fractions were further apart from each other. After incubation the 0.2 µm, 0.45 µm and 1.2 µm filter communities clustered together, while the 12 µm filter communities were less similar.

The bacterial communities of Y3 showed a less distinct grouping after incubation based on the CCA of the samples on gel 2 (Figure 7B). Communities from the same filter fractions before incubation as well as after incubation clustered.

Figure 7C shows the results of the CCA for the bacterial communities of Duvanni Yar. Several clusters could be distinguished. Overall, the pre- and post-incubation samples of Duvanni Yar were distinctive, although there were no clear clusters of samples. Before incubation, the communities from one of the 0.2 µm filters, both 12 µm fractions and one of the 1.2 µm fractions showed similar structures. The other samples before incubation were less similar. The communities after incubation differed from those before incubation. For instance, the 0.45 µm fractions before and after incubation appeared very similar. The post-incubation 12 µm fractions were distinct from the post-incubation cluster.

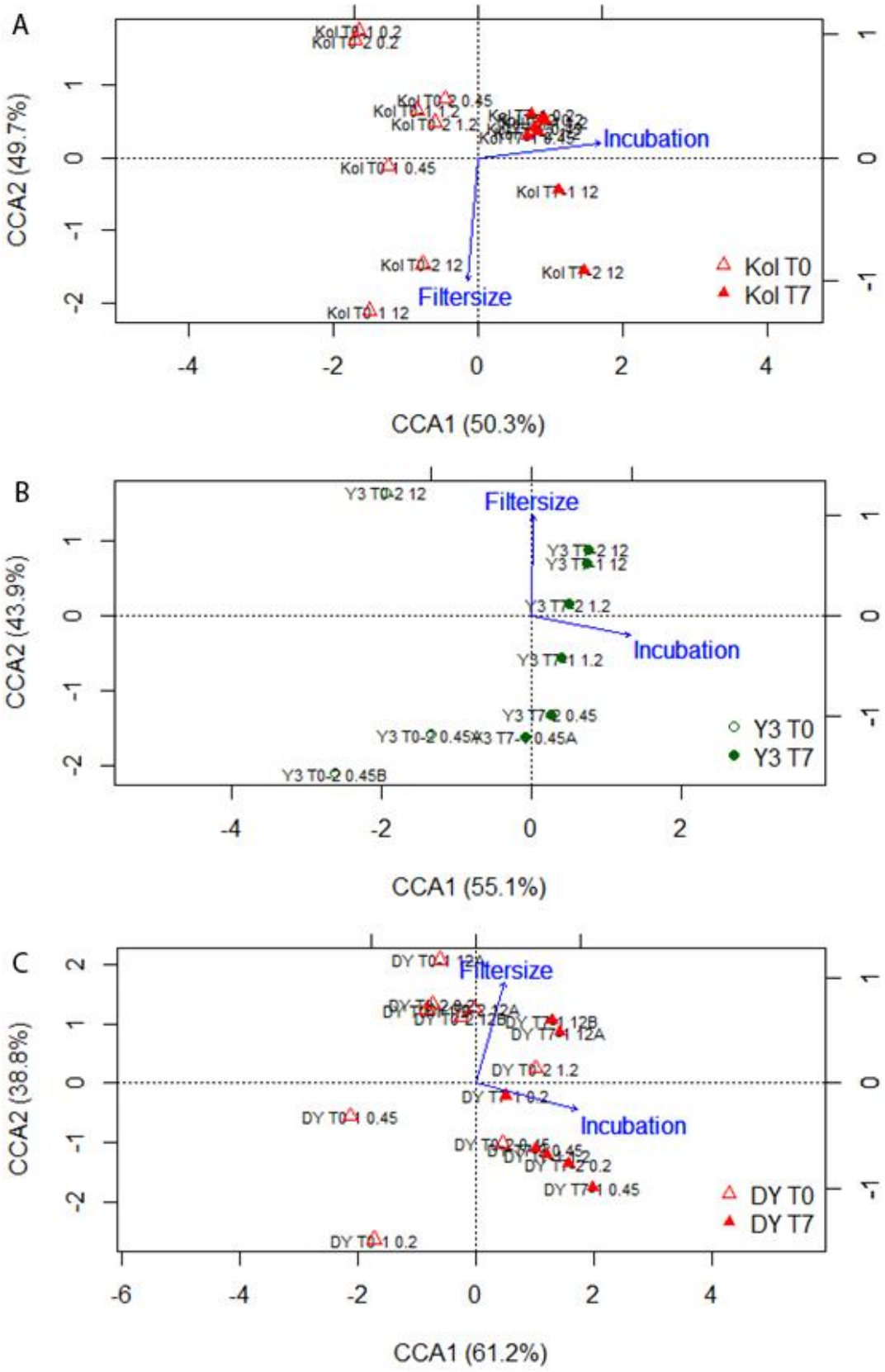

FIGURE 7 ORDINATION PLOT FOR THE FIRST TWO PRINCIPAL DIMENSIONS OF THE RELATIONSHIP BETWEEN BACTERIAL COMMUNITIES OF A) KOLYMA, B) Y3 AND C) DUVANNI YAR.

4.2 Archaea

Here, the results of the DGGEs are described for the archaea, in the same manner as for the bacteria, addressing the first two sub questions of this research.

Figure 8 shows the two DGGE gels with archaeal 16S rRNA gene fragments. The DGGE revealed a wide range of banding patterns in both gels. Most of the darker bands were located in the higher parts of the gel with lower denaturant concentration. Part of the second gel (containing the Duvanni Yar samples) was ignored in further analysis as the lanes with DNA lay on top of each other during the DGGE, as a result of collapsed wells. Per sample, 3 to 17 DGGE bands were detected (see Appendix C for the band quantification matrix).

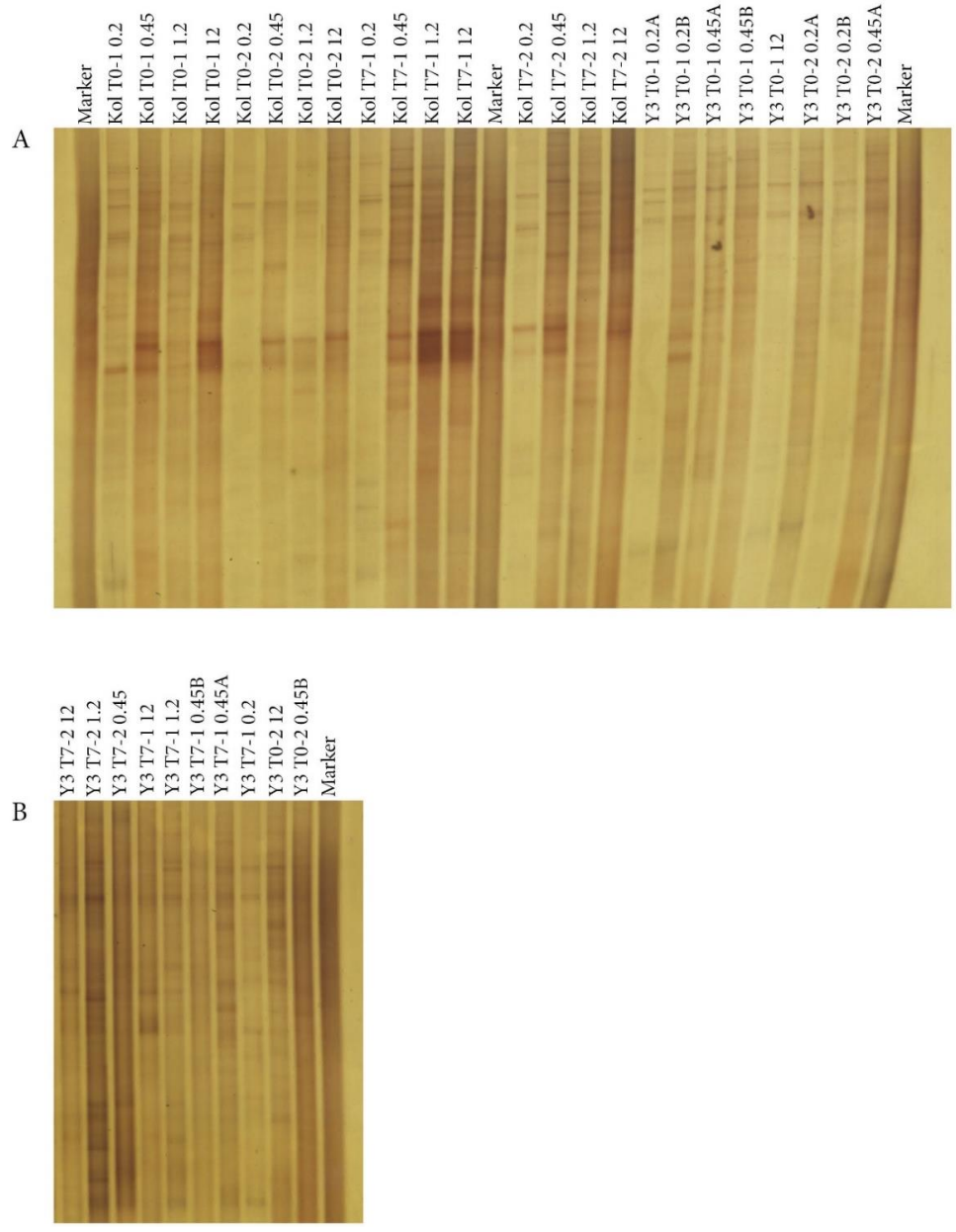

FIGURE 8 DGGE IMAGES OF ARCHAEAL 16S RRNA GENE FRAGMENTS. A) GEL1 AND B) GEL2.

4.2.1 Archaea richness and diversity

The total number of OTUs (richness), the Chao richness estimator and the Shannon diversity (all based on the number of bands on the DGGE gels) before incubation were similar for Kolyma and Y3 (Table 8). After incubation the number of OTUs, the Chao richness estimator and the Shannon diversity showed an increase for Kolyma, but a decrease for Y3.

The four size fractions of Y3 and Kolyma showed diverse patterns in richness and diversity. The number of OTUs of Kolyma showed a decrease after incubation for the 0.2 µm and 12 µm fractions and an increase for the 0.45 µm and 1.2 µm fractions (Figure 9A). The highest pre-incubation number of OTUs was found in the 0.2 µm and 12 µm fractions, whereas after incubation the highest number of OTUs was found in the 0.45 µm fraction. The archaeal Shannon diversity of Kolyma (Figure 9C) showed approximately the same changes after incubation as the number of OTUs, except for the 12 µm fraction, of which the diversity did not change. In general, the Shannon diversity did not show large differences.

The Y3 pre-incubation 1.2 µm filter samples were lacking, as well as one Y3 post-incubation 0.2 µm sample. The other fractions all showed a strong decrease in the number of OTUs after incubation (Figure 9B). The Shannon diversity showed the same patterns (Figure 9D): a decrease after incubation for all analysed size fractions.

TABLE 8 DIVERSITY INDICATORS FOR ARCHAEA FOR KOLYMA AND Y3.

Site	Nr of OTUs (S)		Chao		Shannon (H)	
	Before inc	After inc	Before inc	After inc	Before inc	After inc
Kolyma	54	63	66.4	74.3	3.62	3.79
Y3	50	27	63.3	34.3	3.33	3.00

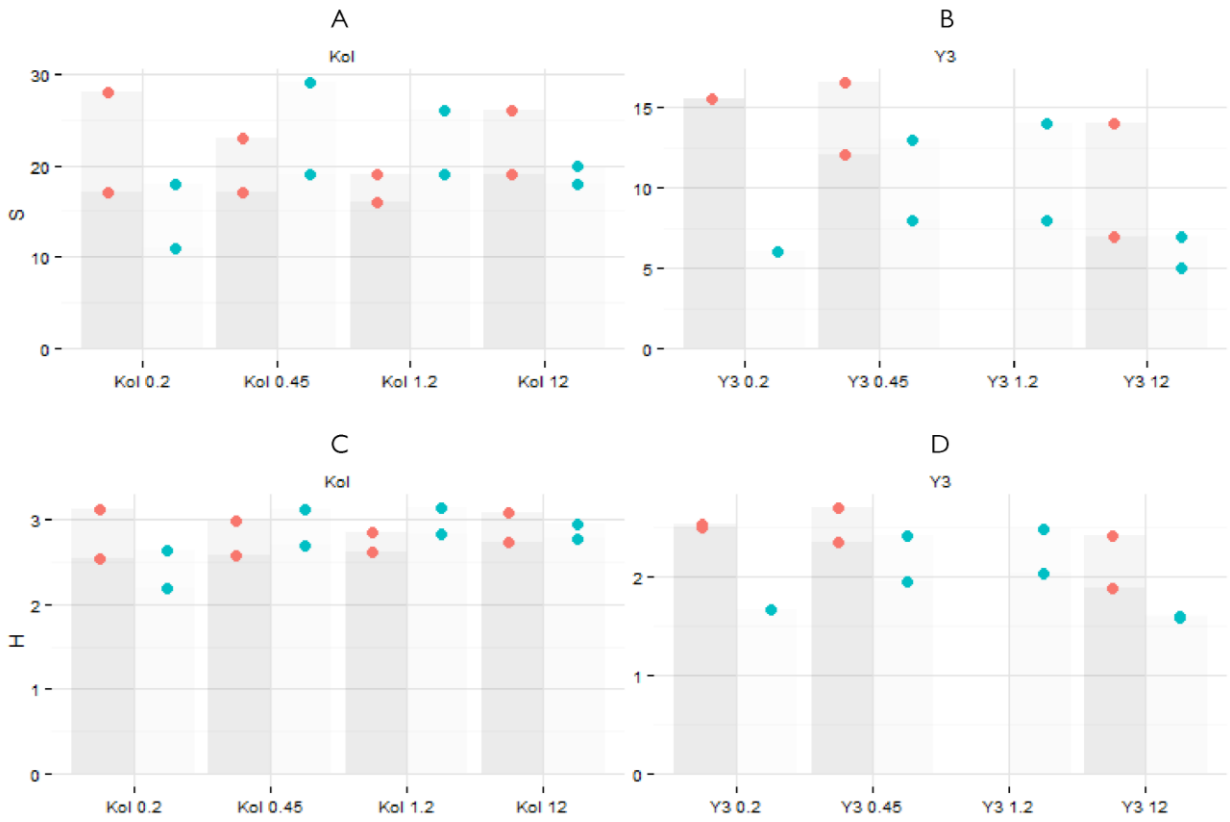

FIGURE 9 SPECIES RICHNESS (S) AND SHANNON DIVERSITY (H) BEFORE AND AFTER INCUBATION FOR KOLYMA (A AND C) AND Y3 (B AND D). PER FILTER, THE VALUES OF THE TWO SAMPLES ARE GIVEN; BEFORE INCUBATION IN RED, AFTER INCUBATION IN BLUE.

4.2.2 Cluster analysis

The UPGMA analysis revealed three major clusters, consisting of Kolyma samples, primarily Y3 pre-incubation samples and mainly Y3 post-incubation samples. Still, some Kolyma samples clustered together with Y3 samples.

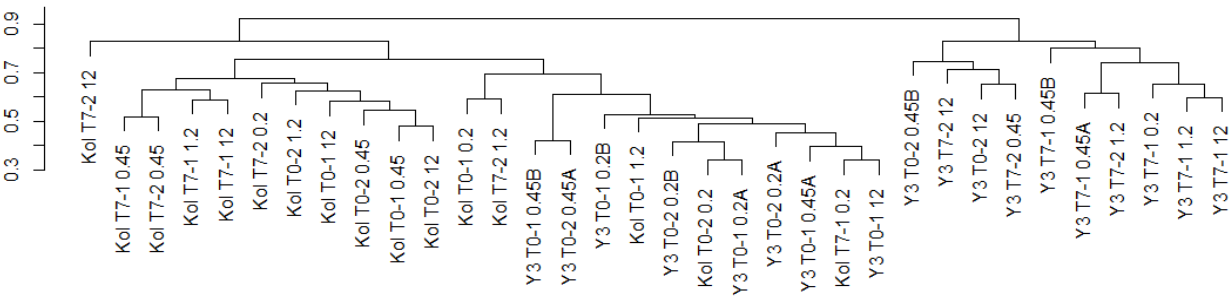

FIGURE 10 UPGMA DENDROGRAM BASED ON THE DGGE BANDING PATTERN OF ARCHAEAL 16S GENE FRAGMENTS.

4.2.3 Constrained analysis of archaeal community composition

Y3 communities before incubation were distinct from those after incubation (Figure 11). The Kolyma communities before and after incubation did not show such a clear difference. The first two CCA axes together explained 84.4 % of the variation in the data. The first axis explained 50.4 % and was mainly linked to site. The second axis explained 34.0 % and was connected to filter pore size and incubation. Site and incubation significantly explained 9.0 % (p = 0.001) and 5.9 % (p = 0.002).

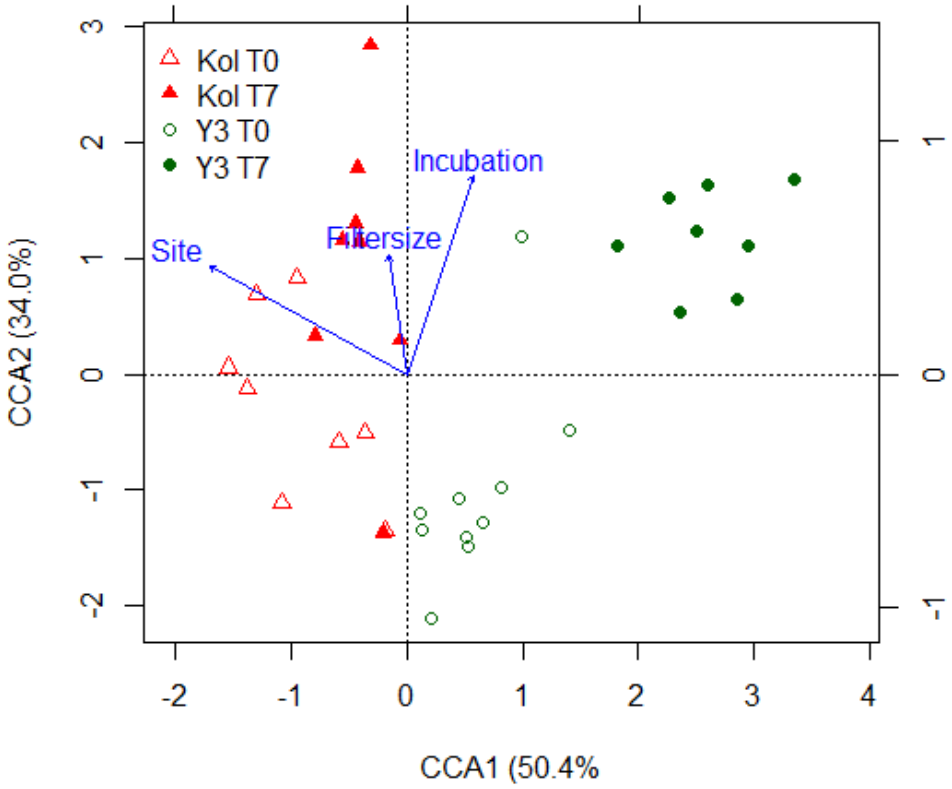

FIGURE 11 ORDINATION PLOT FOR THE FIRST TWO PRINCIPAL DIMENSIONS OF THE RELATIONSHIP BETWEEN ARCHAEAL COMMUNITIES OF KOLYMA AND Y3 AND FILTER PORE SIZE, INCUBATION AND SITE.

Figure 12a shows the result of the CCA of archaeal communities before and after incubation of the Kolyma. Two major groups could be distinguished, the first consisting of the pre-incubation samples and the second of the post-incubation samples. The pre and post incubation 12 µm fractions lay outside the clusters, as well as one post-incubation 0.2 µm sample.

Figure 12b shows the results of the CCA for Y3 and filter pore size and incubation. Two main clusters were distinct. The pre-incubation communities grouped together, except for the 12 µm fractions and one 0.45 µm fraction. After incubation, the 12 µm fractions fell outside the main cluster post-incubation communities.

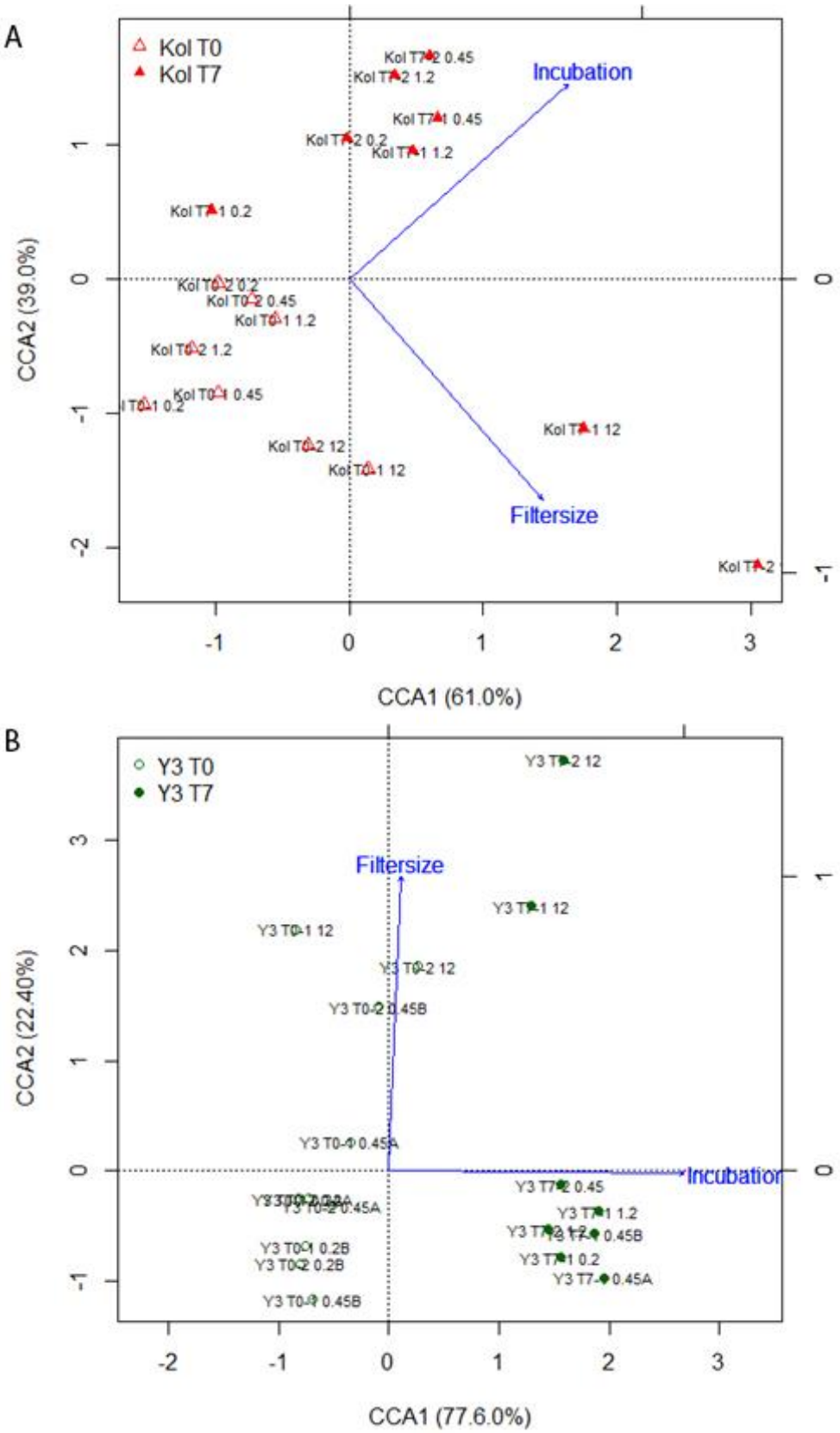

FIGURE 12 CCA PLOT FOR THE FIRST TWO PRINCIPAL DIMENSIONS OF THE RELATIONSHIP BETWEEN ARCHAEAL COMMUNITIES OF A) KOLYMA AND B) Y3 AND FILTER PORE SIZE AND INCUBATION.

4.3 Extracellular enzyme activities

Here, the second research question about nutrient availability in ancient and modern permafrost degradations is addressed. The activities of three hydrolytic and one oxidative enzyme before and after incubation were measured as indication for nutrient availability.

The enzyme assays revealed varying extracellular ß-glucosidase (ß-gluc), n-acetylglucosaminidase (NAG), alkaline phosphatase (Phos) and phenol oxidase (PhOx) activities between Kolyma, Y3 and Duvanni Yar, but also between the four size fractions and before and after incubation (see Appendix D). In general, the extracellular enzyme activities (EEAs) for the 0.2, 0.45 and 1.2 µm fractions were low compared to the extracellular enzyme activities for the 12 µm fractions. Most of the EEA changes after incubation for the 12 µm fractions were significant. Furthermore, the pre-post-incubation changes were generally similar in direction for the different enzymes of one filter pore size. The results are visualized in Figure 13.

4.3.1 ß-glucosidase

The pre-incubation ß-gluc activities lay between 0.0005 (Y3 0.2 µm fraction) and 2.58 nmol hr^{-1} ml^{-1} (Y3 12 µm fraction). After incubation the activities lay between 0 (3 Duvanni Yar samples) and 0.40 nmol hr^{-1} ml^{-1} (Kolyma 12 µm fraction). All Duvanni Yar filters showed a decrease in activity (Figure 13A). All post-incubation activities were undetactable, except for the 12 µm fraction. The decrease in activity for the 12 µm fraction was ($p = 0.0009$). The change in activity was positive for all Kolyma filters, except for the 0.2 µm fraction (Figure 13B). The increase was significant for the 1.2 µm fraction ($p = 0.03574$) and the 12 µm fraction ($p = 0.02021$). For Y3, the 12 µm fraction and the 0.45 µm filter decreased in ß-glucosidase activity, whereas the 0.2 µm filter showed a slight increase (Figure 13C). None of the changes were significant.

4.3.2 N-acetylglucosaminidase

The highest NAG activity before incubation was 0.09 nmol hr^{-1} ml^{-1} (Duvanni Yar 12 µm fraction) and the lowest activity was 0 nmol hr^{-1} ml^{-1} (Duvanni Yar 0.2 µm fraction). After incubation, the NAG activity ranged from 0 nmol hr^{-1} ml^{-1} (Duvanni Yar 1.2 µm fraction and Y3 0.45 µm fraction) to 0.18 nmol hr^{-1} ml^{-1} (Duvanni Yar 12 µm fraction). All pre-incubation EEAs were approximately the same, whereas after incubation Kolyma and Duvanni Yar showed the highest activities and Y3 the lowest activity. For Duvanni Yar, the activities were low for the three 0.2 to 1.2 µm fractions compared to the 12 µm fraction (Figure 13D). The activity increased during incubation for the 0.2 and 12 µm fractions and decreased for the 1.2 µm fraction. The only significant change was the increase in activity for the 12 µm fraction ($p = 0.003467$). The Kolyma 0.2, 0.45 and 12 µm fractions increased in activity, whereas the 1.2 µm fraction showed a decrease in activity (Figure 13E). Y3 showed divergent changes EEA after incubation (Figure 13F). The 0.2 µm fraction increased in activity, whereas the 0.45 and 12 µm fractions showed a decrease in activity. None of the changes of NAG activity for the Kol and Y3 filter fractions were statistically significant.

4.3.3 Alkaline phosphatase

The highest pre-incubation Phos activity was 2.36 nmol hr^{-1} ml^{-1} (Y3 12 µm fraction) and the lowest activity was 0.02 nmol hr^{-1} ml^{-1} (Y3 0.2 µm fraction). After incubation the Phos activity varied between 0.02 nmol hr^{-1} ml^{-1} (Y3 0.45 µm fraction) and 2.4 nmol hr^{-1} ml^{-1} (Kolyma 12 µm filter). Duvanni Yar showed significant but opposite changes for the 1.2 and 12 µm fractions (Figure 13G). The activity decreased during incubation for the 1.2 µm fraction and increased for the 12 µm fraction ($p = 0.003496$). Significant changes

for the Kolyma filters were positive for the 0.2, 1.2 and 12 µm fractions ($p = 0.004734$; $p = 0.0008371$; $p = 0.03235$, respectively) (Figure 13H). Y3 showed significant decreases in activity for the 0.45 and 12 µm fractions ($p = 0.001118$; $p = 0.00002452$, respectively) (Figure 13I). The decrease in activity for the 12 µm fraction was remarkably strong.

4.3.4 Phenol oxidase

Before incubation, the PhOx activity ranged from undetectable (8 samples) to 0.30 µmol hr^{-1} ml^{-1} (Duvanni Yar 12 µm fraction). The post-incubation activities varied between undetectable (10 samples) and 0.42 µmol hr^{-1} ml^{-1} (Duvanni Yar 12 µm fraction). Extracellular PhOx activities for Y3 and Kolyma were undetectable before and after incubation (Figure 13K and Figure 13L). For Duvanni Yar, no PhOx activity was detected for the 0.2 µm fractions, as well as for the post-incubation 0.45 µm fractions (Figure 13J). For the coarser fractions, enzyme activities were detected. Also, PhOx activities were about 1000 times higher than the hydrolytic enzyme activates. Significant changes were positive for the 12 µm faction ($p = 0.03102$).

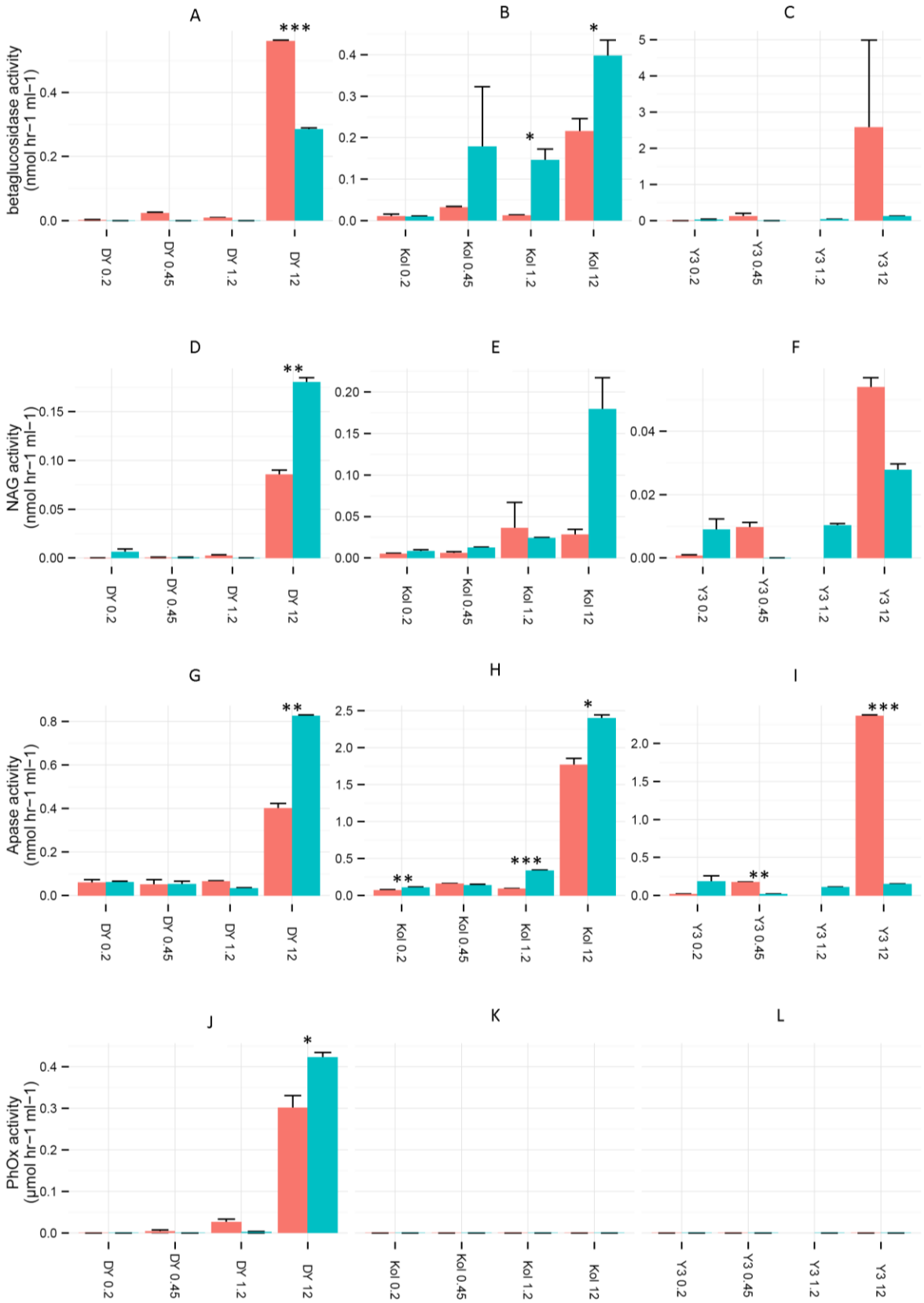

FIGURE 13 ENZYME ACTIVITIES BEFORE (IN RED) AND AFTER INCUBATION (IN BLUE) FOR ALL SITES AND SIZE FRACTIONS. ERROR BARS REPRESENT +1 SE (N

=3). SIGNIFICANT CHANGES ARE INDICATED WITH * (P < 0.05), ** (P < 0.01) OR *** (P <0.001). NOTE DIFFERENT Y-AXIS UNIT FOR PHOX ACTIVITY, AND APASE = PHOS.

5. Discussion

The purpose of this research was to study microbial communities and extracellular enzyme activities (EEAs) originating from aquatic environments dominated by modern (Kolyma and Y3) and ancient carbon (Duvanni Yar) in northeast Siberia, by DNA extraction, PCR and DGGE and enzyme assays. The first aim was to find out if there are differences between bacterial and archaeal richness, diversity and communities in streams and rivers draining modern and ancient carbon. The second aim was to study the effect of a seven-day incubation on the microbial communities. In addition, extracellular enzyme activities were compared between aquatic environments dominated by modern and ancient carbon, as well as before and after incubation.

5.1 Microbial communities

5.1.1 Modern versus ancient carbon dominated waters

Firstly, addressing the comparison in bacterial and archaeal richness and diversity between the studied sites, based on the PCR-DGGE, Duvanni Yar and Kolyma had the same total bacterial richness before incubation, whereas the total bacterial richness of Y3 was lower. The Chao1 richness estimator predicted higher values for the total richness for all sites, but with the same distribution from low to high. The bacterial diversity was highest for Kolyma and lowest for Y3. Duvanni Yars total bacterial diversity lay in between Kolyma's and Y3s diversities. The notion that Y3 had a lower total bacterial diversity and richness than Kolyma and Duvanni Yar before incubation, was also seen in the different filter fractions. However, the 1.2 µm filter was missing for Y3, which could be the cause of the low number of OTUs and diversity compared to the other two sites.

Y3 and Kolyma showed similar archaeal total richness and diversity before incubation. In general there was no clear distinction in initial microbial total richness and diversity between rivers and streams dominated by ancient and modern carbon.

Based on the cluster analysis and the CCAs, the bacterial communities of Kolyma and Y3 were distinct before incubation as well as the archaeal communities of Y3 and Kolyma. Similarly, the pre-incubation bacterial communities of Y3 and Duvanni Yar were distinct. Thus before incubation, Y3 and Kolyma host different initial microbial communities and Y3 and Duvanni Yar host different bacterial communities. The CCAs revealed that the 'site' was for all samples a significant factor in determining the variation. The factor incubation was significant for the bacterial communities analysed on gel1 as well as the archaea.

5.1.2 The effect of incubation

The effect of incubation on the total richness and diversity of microbial communities of the studied sites was not straightforward. Some sites showed either an increase or a decrease in richness and diversity, but there were also sites that showed an increase in richness, while the diversity decreased. For all sites, the total bacterial richness and diversity increased after incubation. The total archaeal richness and diversity increased for Kolyma and decreased for Y3. The change in richness and diversity for the four size fractions

(0.2 µm, 0.45 µm, 1.2 µm and 12 µm) was generally the same as the change in total richness and diversity for the three sites. The separate analysis of the size fractions however also revealed that the large trends were not seen in all size fractions. While some microbial populations profit from the incubation conditions, others do not, or are outcompeted by other microbial populations.

This was also shown by the cluster and CCA analysis. The incubation experiment led to different microbial community compositions between the sites that were compared, and it led to a shift in microbial community composition for each individual site. A remarkable result was that the microbial communities of the 12 µm fractions were after incubation often less similar to microbial communities of the rest of the size fractions of the different sites that were clustered. This implies that the incubation experiment led to a similar microbial community for the smaller size fractions and to a different microbial community in the coarsest fraction.

Bacterial and archaeal richness, diversity and community structure were determined per site, before and after incubation and over four filter fractions (0.2 µm, 0.45 µm, 1.2 µm and 12 µm). The 12 µm filters were often covered with a visible layer of material, while the other filters only showed a slight colouring or even nothing visible with the naked eye. These particles on the 12 µm filters offer a broad spectrum of habitats to microbial organisms. These particle-associated assemblages were, especially after incubation, different from the microbial communities of the finer size fractions which represent free-living bacteria and archaea. This indicates that different processes may play a role in the degradation of particulate organic matter and dissolved organic matter. Hodges et al. (2005) pointed out the importance of particulate organic matter to the pelagic microbial abundance and community structure and carbon cycling. This might also be relevant in the fluviatile environment studied here.

5.1.2 Bacterial versus archaeal richness

The pre-incubation archaeal richness and the Shannon index were higher than the pre-incubation richness and the pre-incubation Shannon indexes. The post-incubation archaeal richness was higher than the bacterial richness for Kolyma and lower for bacterial richness of Y3. The high pre-incubation archaeal richness and diversity compared to the bacterial richness and diversity are in contrast with the hypothesis that the archaeal community is generally less rich and diverse than the bacterial community. The cause for this discrepancy is most likely methodological. First of all, a nested PCR with a total of 65 cycles was applied to amplify the archaeal DNA. This number of cycles is relatively high compared to the number of cycles applied to the bacterial DNA (45) and other studies (30 cycles: Galand et al. 2006; 60 cycles in a nested PCR: Høj et al. 2006). On the one hand this increases the sensitivity and specificity of the reaction, making it possible to visualize rare species (Boon et al. 2002). However, it can also increase the chance of PCR biases (Wintzingerode et al. 1997). It might also be the case that the part of the archaeal community visualised by the DGGE is in fact richer than the part of the bacterial community visualised by the DGGE. One study Galand et al. (2006) has reported on rich archaeal communities. They found rich archaeal communities in the Mackenzie River which might be the result of a primer pair they used, but it could also be related to high particle loads that offer a heterogeneous range of substrates to microbial organisms. However, the archaeal DNA concentrations were low, even after the nested PCR, compared to the bacterial DNA concentrations after the PCR (Appendix F). In fact, since different PCR conditions were applied to amplify the bacterial and the archaeal DNA, a comparison between the results here is

inaccurate. Other techniques in which the amount of microbial DNA is quantitatively assessed (qPCR) or whole environmental genome sequencing allow for the comparison of archaeal and bacterial richness and diversity.

5.1.3 Limitations

Some issues made it difficult and impossible to compare the communities of each site. For the bacterial community fingerprints, 'smiling' of the outermost lanes occurred in the second gel (Figure 3). As the software was unable to correct for this, the four outermost lanes (containing Y3 T0 0.2, Y3 T0 0.45, DY T7 12 and the second DY T7 12 sample) were ignored in the analysis. Furthermore, some samples (Y3 T0 0.2A on gel 1 and Y3 T0 0.2B, Y3 T7-1 0.45B and DY T0 12B on gel 2) did not show any banding pattern and were also neglected. Furthermore, Duvanni Yar samples with archaeal DNA were neglected in the analysis since, as mentioned already in the results, the lanes with banding patterns partially overlapped each other. Consequently, a direct comparison between the bacterial communities of Duvanni Yar and Kolyma was not possible in this study as well as a comparison between the archaeal communities of Y3, Kolyma and Duvanni Yar. It might still be possible that Duvanni Yar and Kolyma have different microbial communities as their environmental conditions are different (Table 1). Y3 and Duvanni Yar hosting different bacterial communities is the only result corroborating the hypothesis that ancient and modern carbon dominated environments host different microbial communities.The DGGE fingerprints provided insight in some of the differences and similarities in microbial communities. However, as it was not possible to make a total comparison of microbial communities of the three sites, no hard conclusions on the differences and similarities can be drawn from the community analysis.

The number of OTUs and the diversity were based on the number of bands per sample, assuming that a single band corresponds to a single OTU. However some species might have more than one 16S gene, thus different bands might represent the same species. And some bands might represent more than one species when their amplified DNA, despite a difference in nucleotide sequences, has an identical migration distance. Although this prevented the estimate of absolute richness and diversity, the samples are treated identically and thus allowed for comparison of the relative richness and diversity within this experiment. A higher number of samples per filter size would have increased the reliability of the results as this would have allowed for statistical analysis (comparison of richness and diversity between sites and before and after incubation).

5.2 Extracellular enzyme activities

In order to find out if the different sites were nutrient limited or not, potential EEAs in pre- and post-incubation samples were measured using high throughput enzyme assays. For all sites, the direction of change in enzyme activity after incubation was generally the same in all size fractions. The highest activities however were found in the coarsest fraction. Furthermore, phenol oxidase (PhOx) activities were undetectable for Kolyma and Y3.

5.2.1 Modern versus ancient carbon dominated waters

Here, the discussion is mainly focused on the activities of the 12 µm fractions, as the activity was highest for these samples and the incubation induced changes were often significant.

Duvanni Yar showed high activities for all measured enzymes before and after incubation. ß-gluc decreased in activity after incubation, whereas NAG, Phos and PhOx increased in activity after incubation. This result contradicts the hypothesis that in Yedoma degradations PhOx activities are low due to a relatively low phenolic content. In contrast with earlier studies on Yedoma degradations where enzyme activities on dissolved organic carbon were measured (Mann et al. 2013, Vonk et al. 2013b), here the enzyme activity is most likely related to particulate organic matter which is retained from the coarsest filter. Hence, it could be the case that the phenolic content in particulate organic matter is higher than in dissolved organic matter. Interestingly, as the activity of hydrolytic enzymes (NAG and Phos) together with PhOx activities, increase with incubation, the phenolic content does not seem to inhibit the degradation of organic carbon here. The increase in Phos and NAG could indicate that P and N become limited during the incubation period.

For Kolyma, again contrasting to Mann et al. (2013), no PhOx activity was detected, while hydrolytic enzyme activities increased (although non-significant for NAG) after incubation. The initial activity and increase in activity of hydrolytic enzymes do not indicate phenolic inhibition in these fractions. As mentioned for Duvanni Yar, it could be that in the Kolyma river, the particulate fraction (or the filter fractions analysed in this study) contains relatively little phenolic compounds. It has been shown by Lobbes et al. (2000) that the particulate fraction of Kolyma water entering the Arctic Ocean, contained less lignin (phenols) than the dissolved organic matter, which indeed could be the case for the organic material on the filters. The increase in hydrolytic enzyme activities could indicate that nutrients become limited during incubation.

For Y3, PhOx activities were below detection limits and the hydrolytic enzymes decreased in activity after incubation (actually, only the Phos activity decrease was significant). Also for Y3, high PhOx activities were expected. Vonk et al. (2013b) found significant positive correlations between enzyme activities (particularly ß-gluc) and organic carbon loss. Therefore the change in enzyme activity between pre and post-incubation could indicate which processes are involved in the degradation of the organic matter. As all hydrolytic enzymes show a decrease in activity, Y3 does not seem to lose much carbon. Apparently, there is no need for extra phosphate or nitrate. Or Y3 waters contain enough nutrients that organic carbon degradation can take place without extra need for nutrients.

In general it seems thus that for the Duvanni Yar meltwater streams, the particulate organic matter studied here contains more phenolic compounds than the dissolved organic matter studied by Mann et al. (2013). The activity of hydrolytic enzymes shows that carbon is degraded at the same time as phenolic reduction takes place. Kolyma's particulate fraction seems to contain less phenolic compounds than the dissolved organic matter as found by Mann et al. (2013). The significant increase in two hydrolytic enzymes may indicate nutrient limitation. Similar to the Kolyma river, the PhOx activities in the Y3 stream were below detection limits, indicating relatively little phenolic compounds in the particulate fractions. However, as hydrolytic enzyme activities decreased, nutrients seemed not limiting. If indeed the particulate organic matter of Duvanni Yar contains more phenolic compounds, than different metabolic processes can be expected in its breakdown. Sinsabaugh et al. (1991) found increasing oxidative enzyme activities with increasing particle size, whereas the largest hydrolytic activities were found in the fractions smaller than 0.2 µm in ephilitic biofilms in a boreal river. In this study, the 12 µm filters of Duvanni Yar

were covered with a clearly visible layer of sediment, while on the 12 µm filters of Kolyma and Y3 the material was only visible as a darker colour.

5.2.2 Limitations

The formula (Equation 3) by Jackson et al. (2013) that was used to calculate enzyme activities from the fluorometric assays contains a factor (mean standard fluorescence) that is used a nominator and later as a denominator. Unfortunately no other formula was found to calculate the EEAs. This might be a problem when comparing the enzyme activities to other studies, but it should not influence the comparison between pre- and post-incubation, size fractions and sites.

The small number of samples (three) did not allow for statistical comparison of all pre- and post-incubation activities, as mentioned in the methods already. A larger number of samples would have increased the reliability of the outcomes as well as increase the chance that samples would have a normal distribution and homoscedasticity and thus allow for parametric tests.

Furthermore, the method of extracting material from filters to determine extracellular enzyme activities has not been found in other literature. It is unclear which part of the material on the filters is found in the water used to measure enzyme activity. Also, parts of the filters themselves might have influenced the fluorescence or absorption, although it was tried to not pipet the visible parts into the wells.

6. Conclusion

Some distinctions in microbial communities between old and modern permafrost degradations were found, though, due to methodological constraints, no direct comparisons could be made. Incubation led for most sites to a convergence of free living microbial community composition and to a different particle associated community.

Extracellular phenol oxidase activities were high for the ancient carbon degradation (Duvanni Yar) and non-detectable for modern carbon degradations (Kolyma and Y3). While phenol oxidase activities increased during incubation, hydrolytic enzyme activities increased as well for Duvanni Yar. Y3 and Kolyma showed opposite patterns for the hydrolytic enzymes, indicating that Kolyma might be limited in nutrients, while in Y3 no extra nutrients are needed.

Enzyme activities were most likely associated with the particulate fraction. The contrasting results of the enzyme assays in comparison with other studies enzyme activities associated with dissolved organic carbon, imply that the particulate organic matter might have a different carbon composition. Therefore the breakdown of this carbon may follow different processes than dissolved organic carbon. The divergence of particle associated microbial communities in comparison to free-living microbial communities corroborates this idea.

7. References

Bertrand, J.C, Caumette, P., Lebaron, P., Matheron, R., Normand, P. and Sime-Ngando, T. (2015) Environmental Microbiology: Fundamentals and Applications – Microbial Ecology. *Springer*, 2015. 933p.

Bell. C.W., Fricks, B.E., Rocca, J.D., Steinweg, J.M., McMahon, S.K. and Wallenstein, M.D. (2013) High-troughput flourometric measurement of potential soil extracellular enzyme activities. *Journal of Visualized Experiments*, **81**. Published online 2013 Nov 15.

Boon, N., de Windt, W., Verstraete, W. and Top, E.M. (2002) Evaluation of nested PCR-DGGE (denaturing gradient gel electrophoresis) with group-specific 16S rRNA primers for the analysis of bacterial communities from different wastewater treatment plants. *FEMS Microbial Ecology* **39**, 101-112.

Crump, B.C., Amaral-Zettler, L.A. and Kling, G.W. (2012) Microbial diversity in arctic freshwaters is structured by inoculation of microbes from soil. *The ISME Journal* **6**: 1629-1639.

Duarte, S., Cassio, F. and Pascoal, C. (2012) Denaturing Gradient Gel Electrophoresis (DGGE) in Microbial Ecology - Insights from Freshwaters, Gel Electrophoresis - Principles and Basics, Dr. Sameh Magdeldin (Ed.), ISBN: 978-953-51-0458-2, InTech, Derived from: http://www.intechopen.com/books/gelelectrophoresis-principles-and-basics/denaturing-gradient-gel-electrophoresis-dgge-in-microbial-ecology-insights-from-freshwaters

Galand, E. P., Lovejoy, C. and Warwick, F.V. (2006) Remarkably diverse and contrasting archaeal communities in a large arctic river and the coastal Arctic Ocean. *Aquatic Microbial Ecology* **44**, 115-126.

Graham, D.E., Wallenstein, M.D., Vishnivetskaya, T.A., Waldrop, M.P., Phelps, T.J., Pfiffner, S.M., Onstott, T.C., Whyte, L.G., Rivkina, E.M., Hettich, R.L., Wagner, D., Wullschleger and S.D., Jansson, J.K. (2012) Microbes in thawing permafrost: the unknown variable in the climate change equation. *The ISME Journal* **6**: 709-712.

Hill, B., Elonen, C.M., Seifert, L.R., May, A.A. and Tarquinio, E. (2012) Microbial enzyme stoichiometry and nutrient limitation in US streams and rivers. *Ecological Indicators* **18**, 540-551.

Hodges, L.R., Bano, N., Hollibaugh, J.T. and Yager, P.L. (2005) Illustrating the importance of particulate organic matter to pelagic microbial abundance and community structure. *Aquatic Microbial Ecology* **40**, 217-227.

Høj, L., Rusten, M., Haugen, L.E., Olsen, R.A. and Torsvik, V.L. (2006) Effects of water regime on archaeal community composition in Arctic soils. *Environmental Microbiology* **8**, 984-996.

IPCC (2014) Climate Change 2014: Synthesis Report. Contribution of Working Groups I, II and III to the Fifth Assessment Report of the Intergovernmental Panel on Climate Change [Core Writing Team, R.K. Pachauri and L.A. Meyer (eds.)]. IPCC, Geneva, Switzerland, 151 pp.

Jackson, C.R., Tyler, H.L. and Millar, J.J. (2013) Determination of Microbial Extracellular Enzyme Activity in Waters, Soils and Sediments using High Throughput Microplate Assays. *Journal of Visualized Experiments* **80**.

Jansson, J.K. and Taş, N. (2014) The microbial ecology of permafrost. *Nature* **12**, 414-425.

Judd, K.E., Crump, B.C. and Kling, G.W. (2006) Variation in dissolved organic matter controls bacterial production and community composition. *Ecology* **87-8**, 2068-2079.

Krivushin, K., Kondrashov, F., Shmakova, L., Tutukina, M., Petrovskaya, L. and Rivkina, E. (2015) Two Metagenomes from Late Pleistocene Northeast Siberian Permafrost. *Genome Announcements* **3-1**, 1-2.

Lobbes, J.M., Fitznar, H.P. and Kattner, G. (2000) Biogeochemical characteristics of dissolved and particulate organic matter in Russian rivers entering the Arctic Ocean. *Geochimica et Cosmochimica Acta* **64-17**, 2973-2983.

Mackelprang, R., Waldrop, M.P., DeAngelis, K.M., David, M.M., Chavarria, K.L., Blazewicz, S.J., Rubin, E.M. and Jansson, J.K. (2011) Metagenomic analysis of a permafrost microbial community reveals a rapid response to thaw. *Nature* **480**, 368-371.

Mann, P.J., Davydova, A., Zimov, N., Spencer, R.G.M, Davydov, S., Bulygina, E., Zimov, S. and Holmes, R.M. (2012) Controls on the composition and lability of dissolved organic matter in Siberia's Kolyma River basin. *Journal of Geophysical Research* **117**, G01028, doi:10.1029/2011JG001798.

Mann, P.J., Sobczak, W.V., Larue, M.M., Bulygina, E., Davydova, A., Vonk. J.E., Schade, J., Davydov, S., Zimov, N., Holmes, R.M., Spencer, R.G.M. (2013) Evidence for key enzymatic controls on metabolism of Arctic river organic matter. *Global Change Biology* **40**, 1089-1100.

Muyzer, G., De Waal, E.C. and Uitterlinden, A.G. (1993) Profiling of Complex Microbial Populations by Denaturing Gradient Gel Electrophoresis Analysis of Polymerase Chain Reaction-Amplified Genes Coding for 16S rRNA. *Applied and Environmental Microbiology* **59-3**, 695-700.

Muyzer. G. (1999) DGGE/TGGE a method for identifying genes from natural ecosystems. *Current opinion in Microbiology* **2**, 317-322.

Ocksanen, J., Blanchet, F.G., Kindt, R., Legendra, P., Minchin, P.R., O'Hara, B., Simpson, G.L., Solymos, P., Stevens, M.H.H. and Wagner, H. (2015) vegan: Community Ecology Package: http://cran.r-project.org/web/packages/vegan/.

Rivkina, E., Gilichinsky, D., Wagener, S., Tiedje, J. and McGrath, J. (1998) Biogeochemical activity of anaerobic microorganisms from buried permafrost sediments. *Geomicrobiology Journal* **15-3**, 187-193.

Schuur, E.A.G., Bockheim, J., Canadell, J.G., Euskirchen, E., Field, C.B., Goryachkin, S.V., Hagemann, S., Kuhry, P., Lafleur, P.M., Lee, H., Mazhitova, G., Nelson, F.E., Rinke, A., Romanovsky, V.E., Shiklomanov, N. Vogel, J.G. and Zimov, S.A. (2008) Vulnerability of Permafrost Carbon to Climate Change: Implications for the Global Carbon Cycle. *BioScience* **58**: 701-714.

Schuur, E.A.G., McGuire, A.D., Schädel, C., Grosse, G., Harden, J.W., Hayes, D.J., Hugelius, G., Koven, C.D., Kuhry, P., Lawrence, D.M., Natali, S.M., Olefeldt, D., Romanovsky, V.E., Schaefer, K., Turetsky, M.R., Treat, C.C. and Vonk, J.E. (2015) Climate change and the permafrost carbon feedback. *Nature* **520**, 171-170.

Shukla, G. and Varma, A. (2011) Soil Enzymology, Soil Biology 22, *Springer*, 2011, 392p.

Sinsabaugh, R.L., Repert, D., Weiland, T., Golladay, S.W. and Linkins, A.E. (1991) Exoenzyme accumulation in epilithic biofilms. *Hydrobiologia* **222**, 29-37.

Sinsabaugh, R.L., Hill, B.H. and Follstad Shah, J.J. (2009) Ecoenzymatic stoichiometry of microbial organic nutrient acquisition in soil and sediment. *Nature* **462**, 795-798.

Sinsabaugh, R.L. (2010) Phenol oxidase, peroxidase and organic matter dynamics of soil. *Soil Biology & Biochemistry* **42**, 391-404.

Spencer, R.G.M., Mann, P.J., Dittmar, T., Eglinton, T.I., McIntyre, C., Holmes, R.M., Zimov, N. and Stubbins, A. (2015) Detecting the signature of permafrost thaw in Arctic rivers. *Geophysical research Letters* **42**. Published online: 27 April 2015.

Vasil'chuk, Y.K. and Vasil'chuk, A.C. (1997) Radiocarbon dating and oxygen isotope variations in the late Pleistocene syngenetic ice-wedges, Northern Siberia. *Permafrost and Periglacial Processes* **8-3**, 335-345.

Vonk, J.E., Mann, P.J., Davydov, S., Davydova, A., Spencer, R.G.M., Schade, J., Sobczak, W.V., Zimov, N., Zimov, S., Bulygina, E., Eglinton, T.I. and Holmes, R.M. (2013a) High biolability of ancient permafrost carbon upon thaw. *Geophysical Research Letters* **40**, 1-5.

Vonk, J.E., Mann, P.J., Dowdy, K.L., Davydova, A., Davydov, S.P., Zimov, N., Spencer, R.G.M., Bulygina, E.B., Eglinton, T.I. and Holmes, R.M. (2013b) Dissolved organic carbon loss from Yedoma permafrost amplified by ice wedge thaw. *Environmental Research Letters* **8**-3, doi: 10.1088/1748-9326/8/3/035023

Wintzingerode F., van, Göbel, U.B. and Stackebrandt, E. (1997) Determination of microbial diversity in environmental samples: pitfalls of PCR-based rRNA analysis. *FEMS Microbiology Reviews* **21**, 213-229.

Zimov, S.A., Davydov, S.P., Zimova, G.M., Davydova, A.I., Schuur, E.A.G., Dutta, K. and Chapin, F.S. (2006a) Permafrost carbon: Stock and decomposability of a globally significant carbon pool. *Geophysical Research Letters* **33**: L20502.

Zimov, S.A., Schuur, E.A.G. and Stuart Chapin III, F. (2006b) Permafrost and the global carbon budget. *Science* **312**, 1612-1613.

Websites

Colorado State University, 2012, http://enzymes.nrel.colostate.edu, visited on 8.4.2015.

Appendices

Appendix A Bacteria Bandquantification Gel1

	Kol T0-1 0.2	Kol T0-1 0.45	Kol T0-1 1.2	Kol T0-1 12	Kol T0-2 0.2	Kol T0-2 0.45	Kol T0-2 1.2	Kol T0-2 12	Kol T7-1 0.2	Kol T7-1 0.45	Kol T7-1 1.2	Kol T7-1 12	Kol T7-2 0.2	Kol T7-2 0.45	Kol T7-2 1.2	Kol T7-2 12	Y3 T0-1 0.2A	Y3 T0-1 0.45A	Y3 T0-1 0.45B	Y3 T0-1 12	Y3 T0-2 0.2A
9.60%	0	0	0	0	0	0	7	0	0	13.7	16.9	1.6	6	20.3	12.7	0	0	0	0	0	0
12.10%	0	0	0	8	0	0	0	9.3	0	0	0	0	0	0	0	0	0	0	0	0	0
12.90%	0	5.1	3.6	0	0	3.8	0	0	0	0	0	5.4	0	0	1.7	5	2.9	4.4	3.3	5.9	0
14.90%	0	0	0	0	0	0	0	0	0	0	0	0	0	0	0	0	3.2	2	0	0	0
18.90%	0	9	3	0	0	0	0	0	0	0	0	0	0	0	0	0	0	0	0	0	0
20.10%	0	0	0	0	0	4	0	0	13	0	0	0	8	4	0	0	0	0	0	0	0
20.80%	0	5.1	3	0	0	0	5	0	11.7	2.1	3	2.8	9.1	0	1	3	4.2	2	0	14	0
21.80%	0	0	0	0	2.4	0	0	0	0	0	0	0	0	0	0	0	0	0	3.1	0	0
22.30%	0	0	0	4	0	0	0	0	0	0	0	0	0	0	0	0	0	0	0	0	0
24.20%	0	0	0	0	0	0	0	0	0	0	0	0	0	0	0	0	0	0	0	0	0
25.40%	0	0	0	0	0	0	0	0	0	0	0	0	2.9	2.1	3.2	0	4	3.2	0	0	0
26.70%	0	2	1	0	0	0	0	0	0	0	0	0	0	0	0	0	0	0	0	0	0
28.70%	0	0	0	0	0	0	19.8	6.3	3	0	6	3.2	2.5	3.7	3	0	0	0	0	1.9	0
31.30%	0	1	5	0	0	0	9.9	6.1	0	9.2	2.4	0	0	4	0	0	0	0	0	0	0
33.50%	0	0	0	6	0	0	0	0	0	3	6	0	0	0	0	0	0	0	0	8	0
34.50%	0	0	0	0	6.3	0	0	4.7	11	2.8	8	6.1	0	0	0	2.6	0	0	0	0	0
35.70%	3	0	0	0	0	0	0	0	15.4	0	0	5.6	6.1	0	0	0	4	1.1	3	0	3.8
37.10%	0	0	0	2.9	0	0	0	0	0	0	0	0	0	0	0	0	0	0	0	0	0
38.50%	0	3.8	2	0	0	0	0	10	2	3	3	0	0	0	0	10	11.3	11	2.9	4	7.1

38.80%	16.3	0	0	0	0	0	0	0	0	0	0	3.6	0	0	0	4	0	0	0	0	0	0
43.40%	0	0	0	0	0	0	0	0	0	0	0	0	2.6	0	0	0	0	0	0	0	9	2
44.60%	0	5.7	0	19.8	0	0	0	8.2	2.3	0	0	0	0	0	0	0	0	0	0	0	0	0
46.00%	0	10.9	0	42	0	0	0	14.2	0	7	0	0	0	0	0	0	0	0	0	0	0	0
47.30%	0	0	0	0	14.9	0	0	0	0	0	0	0	0	0	7	0	0	0	3	3	0	3.2
48.70%	0	0	0	0	0	0	0	0	4.5	0	0	0	4.3	0	0	0	0	0	0	0	0	0
49.70%	0	0	0	0	0	0	0	0	0	0	0	0	2.3	0	0	0	5	0	0	0	0	0
51.10%	29	8	5	0	34.6	13	12	5	9	3.8	12.1	0	0	3.5	9.4	0	12	17.4	16	4.9	8.5	
52.40%	0	0	0	10.7	0	0	0	6.1	6.8	23	40	5	0	3	9.6	8.3	0	0	0	14.8	0	
53.50%	10.2	0	2	0	16	0	0	0	0	0	0	0	0	0	0	0	0	0	0	0	0	0
55.00%	0	0	0	0	0	2	8	13.1	0	1.2	0	0	2.4	8	2.2	0	2.1	1	0	0	0	
56.80%	0	0	0	0	0	0	0	0	0	3	12	0	0	0	3	0	12	0	0	0	0	
57.50%	0	0	0	0	0	0	0	0	0	0	0	0	0	0	0	2.4	0	9	0	0	12	
58.80%	0	0	4	0	0	0	0	0	0	0	0	0	0	0	0	0	0	0	0	0	0	
61.70%	0	0	0	0	0	0	0	0	0	0	0	0	0	0	0	7	2	2.6	0	0	0	
63.70%	0	1.8	4	2	0	0	4	0	0	1.4	5.8	1.5	4.3	30.9	23	35.9	11	6	0	0	5	
65.60%	0	0	0	0	0	0	0	0	13.7	0	0	0	0	0	0	13.1	0	0	0	0	0	
67.00%	7	0	0	0	2	11.8	8	4.4	19.5	0	0	0	0	0	0	0	0	0	0	0	0	
67.80%	0	7.4	11	4	0	10.4	8	0	9.6	15	14	2.6	16.6	13	9.8	0	0	0	0	0	0	
69.00%	0	0	0	0	0	0	0	25.9	0	0	0	0	7.6	0	0	12.5	2.9	4	2.1	16.9	0	
70.60%	0	0	0	0	3	12.2	3	20.9	2.8	0	0	0	0	11	15.9	13	8	8.5	1.8	16.7	2.5	

72.80%	0	0	0	0	0	0	0	0	0	0	0	0	0	0	0	0	2	20.2	13.7	0	0	2.1
74.90%	0	0	0	0	0	0	0	0	0	0	0	0	0	0	0	0	0	34.1	21.8	0	0	8.5
82.30%	0	1.1	8	14.5	0	0	19	10	0	0	2.6	1.6	3.8	3	0	0	0	0	0	0	0	0

Appendix B Bacteria Bandquantification Gel2

	DY T0-1 0.2	DY T0-1 0.45	DY T0-1 1.2	DY T0-1 12A	DY T0-2 0.2	DY T0-2 0.45	DY T0-2 1.2	DY T0-2 12A	DY T0-2 12B	DY T7-1 0.2	DY T7-1 0.45	DY T7-1 1.2	DY T7-1 12A	DY T7-1 12B	DY T7-2 0.2	DY T7-2 0.45	Y3 T0-2 0.45A	Y3 T0-2 0.45B	Y3 T0 -2 12	Y3 T7-1 0.45A	Y3 T7 -1 1.2	Y3 T7 -1 12	Y3 T7-2 0.45	Y3 T7 -2 1.2	Y3 T7 -2 12
9.30%	6	0	0	0	0	0	0	0	0	0	0	0	0	0	0	0	0	0	2	0	3.3	0	0	2	4
12.20%	59	2.5	11	0	2.4	3	3	0	0	0	2.8	4	4	2	3	0	0	3.3	0	0	0	0	0	0	0
14.20%	0	0	0	0	0	0	0	0	0	0	0	0	0	0	0	0	0	0	0	0	0	7	0	3.4	5
16.10%	11	12	17	17	8	15	22	17	20	19	1.4	6	30.3	25.2	5.8	15.1	3.2	0	0	0	2	1.9	11	3	2
18.00%	5.4	2	0	0	0	0	0	0	0	0	0	0	0	0	0	0	0	0	0	0	6.1	2	11.9	4	0
18.90%	17	12 2.6	2.4	6	2.2	1.8	0	2	5	5	0	0	7.4	6.4	2	0	0	0	0	0	11.1	0	21	1.6	0
20.20%	0	6	4	8.7	1.9	2	5	3	1.2	2	0	0	17.5	10	0	3	0	0	0	0	0	6	0	0	8.1
22.10%	0	-29.08	0	0	0	0	0	0	0	0	0	0	0	0	0	0	0	3.1	1.9	0	14.7	29	0	30	29
22.70%	0	10	12.8	44	28	0	0	23	16.7	21.2	2	0	4	9	3.2	0	3.2	0	0	0	0	0	7.8	0	0
23.60%	6.7	7	19.6	21.4	11.2	0	2.6	0	12	8.3	0	0	2.6	8	0	0	0	0	0	0	10	7	0	10.9	14.9
24.60%	24	0	0	0	0	0	0	0	0	0	0	0	0	0	0	0	0	0	9.9	0	18	11	31	0	0
26.9	2	0	3	5.1	7	20	11	12	7	2.4	16.5	21	13	11	17	11	5	0	0	19	2	0	0	0	0

0%																								
28.50%	6.7	0	0	0	0	4	0	0	9	7	0	3	0	0	0	0	2	0	7	0	5	7.1	9	7.2	7.8
29.70%	0	2	1.9	5	0	8	6	3.8	3.1	3	3.2	9	5.5	0	0	0	0	0	0	8	0	11.9	3.1	14	17.2
30.10%	0	0	0	0	0	0	0	0	0	0	0	0	12	6.1	3.2	4.3	0	0	0	0	0	0	0	0	0
31.40%	0	0	0	0	2.2	7	5	4	2	0	9	7	3.9	4	9	3	0	0	0	7	0	0	0	0	0
32.90%	5.6	0	0	0	0	0	0	0	0	0	4	0	0	0	0	0	0	0	9	0	6	11.6	6	16	29
33.60%	0	3.4	10.6	12	4	8	0	7	4	4	0	5	0	0	0	0	2.1	0	0	6	0	0	0	0	0
34.30%	2.7	0	0	0	0	0	6	0	0	0	6	0	6	9	7	5.2	0	0	0	0	0	0	0	4	0
35.90%	2.1	0	2	3.7	0	0	2	3	2.7	4	4	3	2	20	4	2.2	0	3	0	3	0	0	0	0	0
38.20%	0	0	0	0	0	0	1.1	0	0	2.9	4	2.6	4	0	0	0	0	2.9	0	3	0	0	0	0	0
41.00%	0	0	0	2.8	2.9	12	7	10	6	3.7	13	12	8	5.2	3.1	0	0	0	14.1	9	3	0	4.4	0	0
41.90%	6	0	0	0	0	6.7	0	0	0	0	0	5	0	0	10.3	16	0	0	0	4	0	0	0	0	0
43.80%	4.8	2.9	3.3	4	0	0	0	1.9	0	0	0	3	9	4.2	0	0	7	0	2.5	0	2	4	4	0	5
45.8	0	0	0	0	0	5	0	0	0	0	0	0	0	0	0	0	0	0	5.9	0	0	0	0	0	0

0%																								
46.80%	0	0	0	0	0	0	0	4.3	3.9	6.9	6.3	0	0	0	2	0	0	3	0	0	3	0	8	0	0
47.90%	11	0	0	0	0	6	0	0	0	0	0	6	2	4.7	0	6.8	0	0	0	0	0	0	0	0	0
50.40%	0	0	0	0	0	0	0	0	0	0	4.9	0	0	0	0	0	7	16	0	0	0	0	0	6	0
52.30%	0	17.2	23	17.7	38.6	5	7	17.8	14.4	17.9	0	0	0	14.9	5.2	27.9	0	0	0	0	0	0	0	0	0
54.80%	0	12.8	12	19.1	18.5	0	0	21	15.5	17.4	0	0	0	0	0	10	0	0	24.2	0	1	5.6	0	6	9.8
57.10%	0	0	0	0	0	0	0	0	0	8.9	0	0	0	0	0	0	0	0	0	5.9	2	30.4	0	8.3	29.8
63.00%	12	0	0	0	0	0	0	0	0	2	1.8	1.9	3	0	0	0	0	0	0	0	6	18	10	1	16.5
68.80%	0	0	0	0	0	0	0	0	0	0	0	0	0	0	0	0	0	0	0	0	2.1	0	8	1	0
70.50%	10	0	0	0	0	0	0	0	0	0	0	0	0	2.5	2.9	3.3	0	2.1	0	0	0	1	0	0	0
72.30%	0	0	0	0	0	0	0	0	2	5.9	0	0	0	0	0	0	0	1.8	0	0	0	0	0	0	0
73.90%	0	0	0	0	0	0	0	0	0	0	0	0	0	0	0	0	0	0	0	0	0	0	5	2	0
75.10%	4.6	0	0	0	0	0	0	0	0	0	0	0	2.5	0	0	2.6	7	0	0	0	3.1	3	0	0	0
76.3	0	0	0	0	0	0	0	0	0	0	3.1	4	0	0	0	0	0	0	47	0	0	0	0	0	0

0%																									
78.90%	0	0	0	0	0	3	0	0	0	8	0	0	0	0	0	4	0	0	0	5.9	0	0	0	0	0
81.20%	0	0	0	0	0	0	0	0	0	0	0	0	0	3	0	0	0	0	0	0	0	0	0	0	0
82.60%	0	0	0	0	0	0	0	0	0	5	0	0	0	0	0	0	0	0	0	0	0	0	0	0	0

Appendix C Archaea Bandquantification

Sample	KolT0-10.2	KolT0-10.45	KolT0-11.2	KolT0-112	KolT0-20.2	KolT0-20.45	KolT0-212.2	KolT0-2122	KolT0-212	KolT7-10.2	KolT7-10.45	KolT7-11.2	KolT7-112	KolT7-20.2	KolT7-20.45	KolT7-212.2	KolT7-2122	KolT7-212	Y3T0-10.2A	Y3T0-10.2B	Y3T0-10.45A	Y3T0-10.45B	Y3T0-112	Y3T0-20.45A	Y3T0-20.45B	Y3T0-20.2B	Y3T0-20.2A	Y3T0-2122	Y3T0-212.2	Y3T7-10.45A	Y3T7-10.45B	Y3T7-112.2	Y3T7-1122	Y3T7-20.45	Y3T7-212.2	Y3T7-2122
2.20%	0	0	0	0	0	0	0	0	1	3	0	0	0	2	0	0	0	0	0	0	0	0	0	0	0	0	2	0	0	0	3	1	1	13	0
3.50%	0	0	0	0	0	0	4	0	0	0	0	0	0	0	0	0	0	0	0	0	0	0	0	0	0	0	0	0	0	0	0	0	1.7	0	0
5.00%	0	3.1	0	2.9	1	1	0	0	0	0	0	4	0	0	0	0	0	0	0	0	0	0	0	0	0	0	0	0	0	0	0	0	0	0	0
5.80%	0	0	0	0	0	0	3	0	0	0	0	0	0	0	0	0	0	0	0	0	0	0	0	0	0	0	0	0	11	1.9	0	0	0	3	0
7.50%	3	0	0	0	0	0	0	0	0	0	0	3	0	0	0	0	0	0	0	0	0	0	0	4	0	0	6	0	0	0	0	0	3	0	0
9.20%	0	0	0	2	0	0	0	0	0	0	0	0	0	8	3	3	0	0	0	0	0	0	0	4	0	0	0	0	0	0	0	0	0	0	0
10.40%	3	0	0	0	0	2	0	2.1	0	2	0	0	0	0	0	0	0	0	0	0	0	0	0	0	0	0	0	0	0	0	0	0	0	0	0
11.50%	2	0	0	0	0	0	0	0	0	1.7	0	0	0	0	0	0	0	0	0	0	0	4	0	0	0	0	0	4	0	3.9	7	0	4	0
12.30%	2	0	0	0	0	0	0	0	0	0	3	6	5	0	4.3	0	0	5	0	0	0	0	0	1	0	0	0	0	0	0	0	0	0	0	0
13.9	0	0	0	2.7	1	0	0	0	0	9	0	0	0	6	0	0	0	0	0	0	0	0	0	0	0	0	0	0	0	0	0	0	0	0	0

0%																																					
14.80%	0	0	2	0	0	0	0	1.9	0	0	0	0	0	1.8	3	2	0	0	0	0	0	0	0	0	0	0	0	0	0	0	0	0	0	0	0	3
16.50%	3.9	2.3	3	1.9	1.1	0	0	7	3	3	2.9	3	0	0	4	0	3	0	5	0	6	0	2	0	3	0	6.8	0	2	3.9	12	0	3	0		
17.90%	6.8	0	0	3	2	0	2.2	0	0	0	0	0	0	0	0	0	0	0	6	0	0	0	0	2	0	4	0	5	0	0	0	3	4	0		
19.00%	7	4	3	3	2	3.4	5	0	7	1.8	0	0	0	3	4	0	2.7	4	9	5	5.9	5	0	3	6	0	0	0	0	0	0	0	0	0		
20.10%	0	5	0	4	2	0	0	0	2.8	0	0	0	0	0	0	0	0	0	0	0	5.9	0	0	0	0	0	0	0	0	0	0	0	0	0		
21.00%	3.9	3	0	0	0	0	2	3	0	0	7	0	5	0	0	0	0	0	0	0	0	0	0	0	0	0	0	0	0	0	0	0	0	0		
22.30%	0	2.1	0	0	0	2	0	0	0	13	0	3.9	0	8	4	3	0	3	5	7	0	6	0	2	2	0	0	0	0	0	0	0	0	0		
23.80%	0	0	0	0	0	0	0	0	0	0	2	0	0	0	0	0	0	0	6	2	2	2.4	0	0	0	0	0	0	0	0	0	0	3	0		
24.50%	0	4	5	1.9	0	2	0	0	2	0	0	6	0	0	0	0	0	0	0	0	0	0	0	0	2	0	0	0	0	0	0	0	0	0		
26.30%	7.6	0	0	3	0	0	0	2	0	0	0	6	0	0	1	1	0	6.5	0	2	3	4	0	0	3	0	0	0	0	0	0	0	0	0		
27.	5.7	0	0	4	3	0	0	0	3	0	0	0	0	0	0	0	4	8.6	0	2	0	0	0	3	0	4	0	0	0	0	0	0	0	0		

50%																																					
28.40%	0	6.8	1.4	0	0	3	0	3	0	18	8.9	0	0	13	1	0	0	0	0	2	0	0	0	0	3	0	0	0	0	0	0	0	0	0	0	0
29.50%	2.9	0	0	0	0	0	0	0	0	2	2.9	7	0	0	0	0	0	0	0	0	6	0	2	0	0	2	0	5	0	0	0	2	1.9	0	0	0
30.50%	0	3	0	0	0	0	0	0	0	0	0	0	0	0	4	7	3	0	0	0	0	2.9	0	1.7	0	0	0	0	0	0	0	0	0	0	0	0
32.60%	13	4	0	2	0	7	0	2.9	8.1	7	0	0	0	0	5	0	0	0	0	0	0	0	0	0	0	0	0	0	0	0	0	0	0	0	0	0
33.60%	3.2	5	10.3	0	13	5.8	6	0	14.1	0	5.9	4	10.4	3	10.9	0	11.2	13	14	11	15	6.2	0	7.6	11.3	0	0	0	0	0	0	0	0	0	0	0
34.50%	1.9	7	6.9	3.9	7	3.6	6	0	11.5	5.1	0	0	12	0	0	0	8.1	7	12	3	10.8	5.7	0	5.7	6.9	0	0	0	0	0	0	0	1.9	0		
35.80%	0	0	0	0	0	0	0	0	0	5.8	0	5	0	0	0	0	0	0	0	0	0	0	0	0	0	0	0	3.6	2	0	0	0	0	0		
36.90%	2.2	0	0	4.7	0	2	6.8	2.7	0	0	4	0	0	0	0	6	0	0	0	0	0	0	0	0	0	0	0	0	0	0	0	1	0	0		
38.30%	0	0	5.9	0	0	0	0	0	0	0	0	0	0	0	8	0	12	5	0	0	0	4	0	0	0	0	0	0	0	0	0	0	0	0		
39.20%	0	0	4.2	0	0	0	0	0	0	0	0	8	0	0	0	0	0	5	0	0	0	0	0	0	0	0	0	0	0	0	0	0	0	0		

41.20%	0	5	0	2	0	0	0	3	0	8	7	8	0	13	0	1.9	0	0	0	0	2	0	0	0	0	0	0	0	0	0	0	0	0	0	0	0
42.80%	11.9	0	0	0	0	4	0	0	0	2.9	0	0	0	0	11	0	0	2	0	5.1	0	4.9	0	0	0	0	0	0	0	0	0	0	0	0	0	0
44.70%	13	2	0	3.9	0	1.8	0	3.9	0	0	0	0	3.9	0	0	0	0	0	0	0	0	0	0	0	0	0	0	0	0	0	0	0	0	0	0	0
45.70%	9.9	0	6.6	0	7	0	2.9	1	10.9	3.1	3	4	9.9	5	4.4	3	7.3	10.9	5	8.9	8.1	9	0	6.6	20.3	0	0	0	0	0	0	0	0	0	0	0
47.10%	3	3	8.9	0	8	0	5	3	11.8	5.9	3	0	0	0	0	0	8.8	6.1	9	0	10.9	0	0	6.3	18	0	0	0	0	0	0	0	0	0	0	0
48.10%	0	0	0	7	0	0	0	0	0	0	0	0	15.9	0	9.1	0	0	0	0	0	0	0	0	0	0	0	0	0	0	0	0	0	0	0	0	0
50.10%	0	0	0	0	3	2	2	0	0	2	0	8	0	0	0	0	0	0	0	0	0	0	0	4.9	0	0	0	0	0	0	0	0	0	0	0	0
50.80%	0	4	4	2.3	0	0	0	4.8	0	6	6	0	0	0	0	0	0	2.4	0	0	0	0	0	0	0	0	0	0	0	0	0	0	0	0	0	0
53.30%	0	0	0	0	0	0	0	0	0	0	0	0	0	1	3	4	0	2	0	0	0	3	0	0	0	0	0	0	0	0	3	0	0	0	0	0
54.80%	0	0	0	3	0	0	0	0	5	2	0	0	0	0	0	0	0	1.9	0	4	0	0	0	0	0	0	0	0	0	0	0	0	0	0	0	0
56.7	0	0	0	0	0	0	0	0	0	0	0	0	3.9	0	0	0	0	0	0	0	0	0	0	2.1	3	0	0	0	0	0	0	0	0	0	0	0

0%																																					
57.30%	4.8	4	5	0	0	9	1	2.1	2.8	0	0	0	0	0	4	5	0	0	0	0	1	0	0	0	0	0	0	0	0	0	0	0	0	0	0	0
58.30%	0	0	5.4	1.9	0	0	0	0	0	9.3	0	5	0	0	0	7	0	0	0	0	0	0	0	0	0	0	0	0	0	0	0	0	0	0	0	0
59.10%	6.3	0	0	1.9	3.9	6.1	2	1	0	0	0	0	0	11	5	0	0	0	0	0	0	0	0	3	0	0	0	0	0	0	0	0	0	0	0	0
60.20%	0	0	0	0	0	0	0	0	0	0	3	0	0	0	0	0	0	0	0	0	0	0	0	0	0	0	0	0	0	0	0	0	0	0	0	0
62.40%	0	0	0	0	0	0	0	0	0	0	0	0	0	0	4	0	0	4	0	0	0	0	0	0	0	0	0	0	0	0	0	0	0	0	0	0
64.10%	0	2.1	0	3	0	0	0	0	0	3	2.9	5	0	0	0	4	0	0	0	0	0	0	0	0	0	0	0	0	0	0	0	0	0	0	0	0
65.80%	0	0	0	0	0	0	0	0	0	0	0	0	2	3.2	7	0	0	3	0	7	3	6	0	0	3	0	0	0	0	0	0	0	0	0	0	0
67.90%	4	0	6	1.9	3	0	0	0	6	2	0	0	0	0	0	0	3	0	6	0	0	0	0	0	0	3	0	0	0	0	0	0	0	0	0	0
70.70%	3.2	4.5	0	0	0	0	0	0	0	0	0	0	0	0	0	0	0	0	0	2.9	0	0	1	2.6	0	0	3	0	0	0	0	0	0	0	0	0
72.10%	0	0	0	0	0	0	0	0	0	0	0	0	0	2	0	0	0	3.9	0	0	0	0	0	0	5	3	0	2	1	3	1	2.9	6	1.7		
73.	0	0	4	0	0	0	0	0	0	0	8.9	4.2	0	0	8.9	0	0	3	0	0	0	0	0	0	0	0	2	0	0	0	0	5	0	0		

90%																																					
76.00%	6.8	0	0	5.9	0	0	0	0	0	0	6.2	6.1	0	0	7	0	0	0	8	0	0	2.9	2	0	0	6	0	5	0	0	0	1	6	4		
76.90%	0	2.9	0	0	0	0	0	0	2.9	2.9	0	0	0	0	3	0	3.9	0	0	0	4.9	0	0	0	0	0	0	0	0	0	0	0	0	0		
78.00%	0	0	0	0	0	0	0	0	0	0	0	0	0	0	0	0	0	0	0	0	4.9	0	0	0	0	0	0	0	0	0	0	0	0	0		
79.70%	0	0	0	0	0	0	4	0	0	3	3	0	0	0	0	0	0	0	0	4	0	0	6	3	3	0	0	0	2	1.5	4	2.9	2	2.6	3.9		
80.30%	0	0	0	0	0	0	0	0	0	3	0	4	0	0	0	5	0	0	0	0	0	0	0	0	0	0	0	0	0	0	0	0	0	0	0		
81.90%	0	0	0	0	0	0	0	0	0	3	0	0	0	0	0	0	0	6	0	0	0	0	0	0	0	0	0	0	0	0	0	0	4.9	0			
83.30%	4.2	0	0	0	0	0	0	0	2.2	0	0	0	0	3.9	5	0	0	0	6	3	0	0	0	0	0	0	0	0	0	0	0	0	10.5	0		
84.50%	0	6.8	0	0	2	0	0	4	0	0	0	0	0	0	0	0	0	0	0	0	0	0	0	0	0	0	0	2	2	0	0	0	0	0	0		
86.10%	0	0	0	0	0	0	0	0	0	3.3	0	0	0	0	0	0	0	0	0	0	0	0	0	0	0	0	0	0	0	0	0	0	0	0	0		
87.50%	7	14.9	4	14.9	0	16	10	13	0	14.9	13	11	23	15.1	4	5.9	2	0	0	0	0	0	0	0	0	0	0	0	1	3	0	4	0	0		

89.30%	2.8	0	4	7	1	0	0	0	0	0	0	0	0	0	0	2.9	6.5	0	0	3	3	0	0	0	0	0	0	0	0	0	0	0	0	2	10	0
90.90%	0	0	0	0	0	0	0	0	0	0	0	0	0	0	0	0	10.8	0	0	0	0	0	0	2	2	0	0	0	0	0	0	0	0	0	0	0
92.10%	0	0	0	0	0	0	0	0	0	0	0	0	0	0	0	0	6.9	0	0	0	0	0	0	0	0	2	0	0	3	0	6.1	0	0	0	0	0
93.50%	0	0	0	0	0	0	0	0	0	0	0	0	0	0	0	4	0	0	0	0	0	0	0	0	0	0	0	0	0	0	0	0	0	0	0	0	0
94.80%	0	0	0	0	6	0	0	0	2	6	0	7	0	0	0	0	0	0	6.4	3	0	3	0	0	0	0	0	0	0	0	0	0	0	0	0	0	0
95.90%	0	0	0	6.6	0	7	2	3	0	10	6.4	0	7	11.7	0	0	0	0	0	0	0	0	4	0	3	0	0	0	0	0	0	0	0	0	0	0	0
96.90%	21	8.9	5	0	0	0	0	0	0	0	0	0	0	0	0	0	0	0	0	0	0	0	0	0	0	0	0	0	0	0	0	0	0	0	0	0	0
97.80%	0	0	0	0	0	0	0	0	0	0	0	0	0	0	0	0	0	0	0	0	0	0	0	0	0	0	0	7.7	3.4	0	7.5	0	0	9	0							
98.90%	0	0	0	0	0	0	0	0	0	0	0	0	0	0	0	0	0	0	0	0	0	0	0	0	0	0	0	0	0	0	0	0	6	0	3.1							

Appendix D Enzyme activities

Activity	ß-gluc (nmol hr-1 ml-1)						NAG (nmol hr-1 ml-1)						Phos (nmol hr-1 ml-1)						PHOX (µmol hr-1 ml-1)					
	obs 1	*obs 2*	*obs 3*	*average*	*se*	*sign*	*obs 1*	*obs 2*	*obs 3*	*average*	*se*	*sign*	*obs 1*	*obs 2*	*obs 3*	*average*	*se*	*sign*	*obs 1*	*obs 2*	*obs 3*	*average*	*se*	*sign*
DY T0 0.2	0	0.003865	0.001933	0.001933	0.001116	0.2254	0	0	0	0	0	0.1835	0.033428	0.068945	0.075213	0.059195	0.011301	0.82004	0	0	0	0	0	
DY T0 0.45	0.026403	0.025013	0.016675	0.022697	0.003037	0.01744	0	0.001415	0	0.000472	0.000472	0.4226	0.008734	0.065506	0.078607	0.050949	0.021444	0.92818	0.009664	0.002664	0	0.004109	0.002882	0.29
DY T0 1.2	0.009975	0.00798	0.00798	0.008645	0.000665	0.005865	0	0.00308	0.003696	0.002259	0.001143	0.1869	0.060686	0.068103	0.064732	0.064507	0.002144	0.003496	0.038664	0.017664	0.023664	0.026664	0.006245	0.03094
DY T0 12	0.555294	0.558082	0.566911	0.560096	0.003501	0.00009	0.077263	0.092619	0.08734	0.085741	0.004505	0.003467	0.44448	0.392244	0.367551	0.401425	0.022677	0.003496	0.356664	0.289664	0.258664	0.301664	0.028919	0.03102
DY T7 0.2	0	0	0	0	0		0.009314	0	0.009314	0.006209	0.003105		0.050915	0.065462	0.06728	0.061219	0.005179		0	0	0	0	0	
DY T7 0.45	0	0	0	0	0		0	0.001493	0	0.000498	0.000498		0.023308	0.065262	0.066816	0.051795	0.014251		0	0	0	0	0	
DY T7 1.2	0	0	0	0	0		0	0	0	0	0		0.02528	0.035924	0.035924	0.032376	0.003548		0.005664	0	0	0.001888	0.001888	
DY T7 12	0.288775	0.289988	0.274821	0.284528	0.004866		0.171491	0.176321	0.189743	0.181015	0.004808		0.833727	0.818592	0.823006	0.825109	0.004494		0.443664	0.404664	0.426064	0.429997	0.011319	
Y3 T0 0.2	0	0.001481	0	0.000494	0.000494	0.2982	0.001359	0	0.000679	0.000679	0.000392	0.119	0.021369	0.018611	0.017233	0.019071	0.001216	0.15448	0	0	0	0	0	
Y3 T0 0.45	0.022565	0.031591	0.288832	0.114329	0.087293	0.3216	0.010284	0.011998	0.006856	0.009713	0.001512	0.02338	0.164652	0.17189	0.182746	0.173096	0.005258	0.001118	0	0	0	0	0	
Y3 T0 1.2	0	0	0	0	0																			
Y3 T0 12	0.16452	7.409921	0.161262	2.578568	2.415677	0.4161	0.05086	0.059943	0.05086	0.058388	0.003027	0.005211	2.361487	2.34846	2.383818	2.364588	0.010324	2.45E-05	0	0	0	0	0	
Y3 T7 0.2	0.005257	0.054317	0.007009	0.022194	0.016069		0.015277	0.007639	0.003819	0.008912	0.003368		0.109526	0.113369	0.330498	0.184464	0.073025		0	0	0	0	0	
Y3 T7 0.45	0	0.000745	0.000745	0.000497	0.000248		0	0	0	0	0		0.017952	0.020023	0.018642	0.018872	0.000609		0	0	0	0	0	
Y3 T7 1.2	0.017753	0.037724	0.036245	0.030574	0.006425		0.009569	0.010367	0.011164	0.010367	0.000046		0.109513	0.111946	0.112758	0.111406	0.000975		0	0	0	0	0	
Y3 T7 12	0.123505	0.123505	0.120009	0.12234	0.001165		0.024367	0.030078	0.028215	0.027787	0.001863		0.14479	0.152547	0.149961	0.149099	0.00228		0	0	0	0	0	
Kol T0 0.2	0.003724	0.020481	0.007448	0.010551	0.00508	0.8697	0.004285	0.006428	0.004285	0.005	0.000714	0.03844	0.053853	0.07324	0.079702	0.068932	0.007767	0.004734	0	0	0	0	0	
Kol T0 0.45	0.028593	0.036291	0.030792	0.031892	0.002289	0.419	0.003534	0.005302	0.008836	0.005891	0.001559	0.02219	0.167369	0.152154	0.158916	0.159480	0.004401	0.31992	0	0	0	0	0	
Kol T0 1.2	0.012886	0.008591	0.014318	0.011931	0.001721	0.03574	0.004352	0.006092	0.097478	0.035975	0.030756	0.733	0.087826	0.088704	0.097487	0.091339	0.003084	0.000837	0	0	0	0	0	
Kol T0 12	0.186796	0.182087	0.275055	0.215313	0.030901	0.02021	0.037888	0.030018	0.017153	0.028350	0.006041	0.07604	1.932443	1.651075	1.726059	1.769859	0.084125	0.032350	0	0	0	0	0	

Kol T7 0.2	0.01241 6	0.00886 8	0.00709 5	0.00946	0.00156 4		0.00636 1	0.01060 2	0.00848 1	0.00848 1	0.00122 4		0.08971	0.11534 2	0.11320 6	0.10608 6	0.00821 1		0	0	0	0	0	
Kol T7 0.45	0.03383 1	0.03383 1	0.46719 2	0.17828 5	0.14445 4		0.01165	0.01165	0.01359 1	0.01229 7	0.00064 7		0.11750 9	0.14688 6	0.15472	0.13970 5	0.01132 6		0	0	0	0	0	
Kol T7 1.2	0.09666	0.15626 8	0.18526 6	0.14606 5	0.02608 2		0.02391 5	0.02309 1	0.02556 5	0.02419	0.00072 7		0.32468 6	0.34934 6	0.34030 4	0.33811 2	0.00720 3		0	0	0	0	0	
Kol T7 12	0.32739 8	0.41360 8	0.45397 2	0.39832 6	0.03732 9		0.12013 5	0.16696 8	0.25045 1	0.17918 5	0.03811 2		2.33030 7	2.39632 8	2.47369 5	2.40011	0.04143 6		0	0	0	0	0	

Appendix E Statistics CCAs

Bacteria gel1

```
Accumulated constrained eigenvalues
Importance of components:
                         CCA1   CCA2   CCA3
Eigenvalue            0.4074 0.3261 0.3155
Proportion Explained  0.3884 0.3109 0.3007
Cumulative Proportion 0.3884 0.6993 1.0000


Biplot scores for constraining variables

               CCA1    CCA2     CCA3 CA1 CA2 CA3
Incubation -0.1018 -0.9919  0.07365   0   0   0
Filtersize -0.4272  0.2324  0.87393   0   0   0
Site       -0.8890 -0.3888 -0.24236   0   0   0

Permutation test for cca under reduced model
Terms added sequentially (first to last)
Permutation: free
Number of permutations: 999

Model: cca(formula = bqgel1 ~ Incubation + Filtersize + Site, data = Gel1env)
           Df ChiSquare      F Pr(>F)         % variation explained
Incubation  1   0.32691 2.3071  0.002 **       13.57
Filtersize  1   0.33363 2.3545  0.002 **       13.85
Site        1   0.38850 2.7417  0.001 ***      16.13
Residual   17   2.40888
---
Signif. codes:  0 ‘***’ 0.001 ‘**’ 0.01 ‘*’ 0.05 ‘.’ 0.1 ‘ ’ 1
```

Bacteria gel2

```
Call:
cca(formula = bqgel2 ~ Site + Filtersize + Incubation, data = Gel2env)

Partitioning of mean squared contingency coefficient:
              Inertia Proportion
Total          3.2957      1.000
```

```
Constrained    0.8634      0.262
Unconstrained  2.4323      0.738

Accumulated constrained eigenvalues
Importance of components:
                        CCA1   CCA2   CCA3
Eigenvalue            0.5145 0.1946 0.1474
Proportion Explained  0.6007 0.2272 0.1721
Cumulative Proportion 0.6007 0.8279 1.0000

Biplot scores for constraining variables

              CCA1   CCA2    CCA3 CA1 CA2 CA3
Incubation -0.5024 0.8062  0.3141   0   0   0
Filtersize -0.2894 0.2023 -0.9355   0   0   0
Site        0.9762 0.1841 -0.1126   0   0   0

Permutation test for cca under reduced model
Terms added sequentially (first to last)
Permutation: free
Number of permutations: 999

Model: cca(formula = bqgel2 ~ Site + Filtersize + Incubation, data = Gel2env)
           Df ChiSquare      F Pr(>F)         % variation explained
Site        1   0.49942 4.3119  0.001 ***      20.535
Filtersize  1   0.16129 1.3925  0.197          6.632
Incubation  1   0.20270 1.7501  0.051 .        8.334
Residual   21   2.43228
---
Signif. codes:  0 ‘***’ 0.001 ‘**’ 0.01 ‘*’ 0.05 ‘.’ 0.1 ‘ ’ 1
```

Archaea

```
Accumulated constrained eigenvalues
Importance of components:
                        CCA1   CCA2   CCA3
Eigenvalue            0.3269 0.2201 0.1010
Proportion Explained  0.5044 0.3397 0.1558
Cumulative Proportion 0.5044 0.8442 1.0000


Biplot scores for constraining variables

               CCA1   CCA2    CCA3 CA1 CA2 CA3
Incubation  0.28229 0.8522  0.4431   0   0   0
Filtersize -0.08052 0.5125 -0.8558   0   0   0
Site       -0.84906 0.4662  0.2392   0   0   0


Permutation test for cca under reduced model
Terms added sequentially (first to last)
Permutation: free
Number of permutations: 999

Model: cca(formula = bq ~ Incubation + Filtersize + Site, data = Archaeaenv)
           Df ChiSquare      F Pr(>F)     % variation explained
```

```
Incubation  1    0.2052 1.7745  0.002 **  5.91 %
Filtersize  1    0.1301 1.1245  0.232     3.75
Site        1    0.3127 2.7032  0.001 *** 9.01
Residual   30    3.4699
---
Signif. codes:  0 ‘***’ 0.001 ‘**’ 0.01 ‘*’ 0.05 ‘.’ 0.1 ‘ ’ 1
```

ACCUMULATED CONSTRAINED EIGENVALUES

CCA Archaea Kolyma

```
Importance of components:
                        CCA1   CCA2
Eigenvalue            0.2587 0.1657
Proportion Explained  0.6096 0.3904
Cumulative Proportion 0.6096 1.0000


Permutation test for cca under reduced model
Terms added sequentially (first to last)
Permutation: free
Number of permutations: 999

Model: cca(formula = bq[1:16, ] ~ Incubation + Filtersize, data = Archaeaenv[1:16, ])
           Df ChiSquare      F Pr(>F)
Incubation  1   0.21751 1.3336  0.055 .
Filtersize  1   0.20682 1.2680  0.129
Residual   13   2.12036
```

CCA Archaea Y3

```
Accumulated constrained eigenvalues
Importance of components:
                        CCA1   CCA2
Eigenvalue            0.5975 0.1723
Proportion Explained  0.7762 0.2238
Cumulative Proportion 0.7762 1.0000


Permutation test for cca under reduced model
Terms added sequentially (first to last)
Permutation: free
Number of permutations: 999

Model: cca(formula = bq[17:34, ] ~ Incubation + Filtersize, data = Archaeaenv[17:34,
])
           Df ChiSquare      F Pr(>F)
Incubation  1    0.5975 2.7704  0.001 ***
Filtersize  1    0.1723 0.7990  0.800
Residual   15    3.2352
```

Appendix F

SAMPLE	TOTAL	ARCHAEA		BACTERIA
	DNA conc after isolation ng/µl	DNA conc purified after pcr (16S) ng/ul	DNA conc purified after pcr (16S dgge) ng/ul	DNA conc purified after pcr (16S DGGE) ng/µl
KOL T0-1 0.2	10.90	4.50	9.20	37.70
KOL T0-1 0.45	26.70	5.60	5.50	48.80
KOL T0-1 1.2	18.90	7.30	8.20	35.50
KOL T0-1 12	22.30	5.50	13.40	43.30
KOL T0-2 0.2	1.00	8.80	10.30	29.20
KOL T0-2 0.45	3.10	5.60	16.50	26.20
KOL T0-2 1.2	2.20	4.80	8.50	23.80
KOL T0-2 12	7.30	5.40	14.90	22.20
KOL T7-1 0.2	8.10	6.30	7.00	19.20
KOL T7-1 0.45	10.70	5.40	13.40	24.50
KOL T7-1 1.2	5.60	7.10	13.50	37.70
KOL T7-1 12	15.60	6.50	14.00	20.80
KOL T7-2 0.2	4.50	7.70	4.20	26.30
KOL T7-2 0.45	6.40	5.40	17.90	29.00
KOL T7-2 1.2	3.20	6.50	10.30	44.30
KOL T7-2 12	10.60	5.50	21.50	28.60
Y3 T0-1 0.2A	1.20	6.60	10.40	21.80
Y3 T0-1 0.2B	2.60	9.50	6.40	13.60
Y3 T0-1 0.45A	3.10	4.40	12.20	32.30
Y3 T0-1 0.45B	5.70	5.70	8.70	37.50
Y3 T0-1 12	1.50	6.80	7.90	27.70
Y3 T0-2 0.2A	2.30	6.10	11.90	9.10
Y3 T0-2 0.2B	3.10	6.00	8.30	20.70
Y3 T0-2 0.45A	9.20	6.00	10.80	30.20
Y3 T0-2 0.45B	12.10	5.00	11.30	35.60
Y3 T0-2 12	0.80	4.70	8.4	24.4
Y3 T7-1 0.2	9.70	5.70	6.00	32.70
Y3 T7-1 0.45A	6.00	4.50	8.00	37.70
Y3 T7-1 0.45B	5.30	4.40	22.80	12.50
Y3 T7-1 1.2	4.00	4.20	8.00	19.60
Y3 T7-1 12	4.00	4.80	18.10	13.00
Y3 T7-2 0.45	35.60	5.70	37.10	42.60
Y3 T7-2 1.2	3.50	6.60	9.60	31.60
Y3 T7-2 12	7.70	11.20	23.40	24.30
DY T0-1 0.2	0.30	6.90	11.50	24.50
DY T0-1 0.45	5.30	7.20	13.10	25.30

DY T0-1 1.2	1.60	5.90	7.80	33.10
DY T0-1 12A	4.00	6.40	7.30	9.50
DY T0-1 12B	6.10	5.90	14.00	39.00
DY T0-2 0.2	5.00	7.40	10.50	30.30
DY T0-2 0.45	4.10	6.80	14.90	48.50
DY T0-2 1.2	3.40	7.00	13.90	27.50
DY T0-2 12A	8.90	6.50	22.30	41.40
DY T0-2 12B	27.50	6.90	9.10	39.30
DY T7-1 0.2	1.90	6.30	6.90	19.30
DY T7-1 0.45	3.10	5.20	8.50	41.60
DY T7-1 1.2	0.80	6.20	23.90	33.10
DY T7-1 12A	7.30	13.30	11.30	26.30
DY T7-1 12B	11.00	3.50	10.90	5.60
DY T7-2 0.2	0.30	17.60	11.60	31.20
DY T7-2 0.45	3.50	5.80	13.20	34.00
DY T7-2 1.2	2.10	7.20	7.00	41.20
DY T7-2 12A	25.80	5.00	9.60	41.70
DY T7-2 12B	29.20	6.00	14.00	33.30

Acknowledgements

As the end of my master came closer, I found it was time to choose a topic that always had my interest, but which I never had a chance to work on (except for looking at ice wedge and pingo remnants in the Netherlands): permafrost. I was thinking of the effect of permafrost thaw on vegetation, but Jorien had a project on microbial communities and enzymes in relation to permafrost thaw. It would be a project in which I was unfamiliar with almost everything, and thus a great challenge and opportunity! Henk teached me how to use a pipette, the usual workflow in molecular biology, working as clean as possible to not contaminate samples, labeling samples, all the techniques, etc. which was time consuming as I basically had no lab skills at all, nor a background in molecular biology… Thanks a lot and also for the supervision during the project in Yerseke! Also many thanks to Veronique for the help with the DGGE! Then in Newcastle, where we had to find a way to measure enzyme activities from filters, many thanks to Paul, Sam and Jorien for the discussions and especially Sam for preparing the chemicals and measuring fluorescence and absorbance when I had to catch my flight. During the writing process, getting comments from different readers was sometimes confusing. But Henk, without your eye for detail and perfection, a lot of sentences would still be clumsy or even inaccurate! And Maarten, your comments were helpful to keep the overview and structure! Of course I also have to thank Bas for always being ready to support me and helping me with making my graphs in r, and Albert and Melanie for delivering feedback on the written parts. Jorien, thanks for providing literature when necessary, reading every single part, your enthusiasm and last but not least making it (also financially) possible to go to Yerseke and Newcastle!